

FACILITY FORM 802

N66 37644

(ACCESSION NUMBER)
80
(PAGES)
CR-66164
(NASA CR OR TMX OR AD NUMBER)

(THRU)
1
(CODE)
14
(CATEGORY)

NASA Contractor Report No. 66164

A SYSTEM TO MEASURE THE MASS OF A PROJECTILE LAUNCHED FROM AN EXPLODING FOIL GUN

by

J. A. Morrea

DISTRIBUTION OF THIS REPORT IS PROVIDED IN THE INTEREST OF
INFORMATION EXCHANGE. RESPONSIBILITY FOR THE CONTENTS
RESIDES IN THE AUTHOR OR ORGANIZATION THAT PREPARED IT.

Final Report

Prepared by

AVCO CORPORATION
AVCO SPACE SYSTEMS DIVISION
ENVIRONMENTAL SCIENCES AND TECHNOLOGY DIRECTORATE
Wilmington, Massachusetts

L-5344

Contract NAS1-5221
AVSSD-0222-66-RR

GPO PRICE \$ _____

CFSTI PRICE(S) \$ _____

Hard copy (HC) \$ 2.50

Microfiche (MF) .75

June 1966

ff 653 July 65

Prepared for

NATIONAL AERONAUTICS AND SPACE ADMINISTRATION
LANGLEY RESEARCH CENTER
LANGLEY STATION,
Hampton, Virginia

A SYSTEM TO MEASURE THE MASS OF A PROJECTILE
LAUNCHED FROM AN EXPLODING FOIL GUN

by

J. A. Morreal

DISTRIBUTION OF THIS REPORT IS PROVIDED IN THE INTEREST OF
INFORMATION EXCHANGE. RESPONSIBILITY FOR THE CONTENTS
RESIDES IN THE AUTHOR OR ORGANIZATION THAT PREPARED IT.

Final Report

Prepared by

AVCO CORPORATION
AVCO SPACE SYSTEMS DIVISION
ENVIRONMENTAL SCIENCES AND TECHNOLOGY DIRECTORATE
Wilmington, Massachusetts

L-5344
Contract NAS1-5221
AVSSD-0222-66-RR

June 1966

Prepared for

NATIONAL AERONAUTICS AND SPACE ADMINISTRATION
LANGLEY RESEARCH CENTER
LANGLEY STATION,
Hampton, Virginia

ABSTRACT

The design of a projectile-mass measuring system is discussed. The primary mechanism is an inverted thrust table using flat spring flexures with strain gage readout to measure the momentum transfer from a projectile of unknown mass but known velocity. A mass range of from 2 to 30 mg with a velocity range of from 6 to 15 km/s can be accommodated.

EDITED BY:
EDITORIAL SERVICES SECTION
J. J. MCCARRON

CONTENTS

1.0	Summary	1
2.0	Introduction.....	2
3.0	Theoretical Considerations	3
3.1	Mechanical Design of Thrust Table.....	4
3.2	Final Mechanical Design	5
3.3	Multiplate Target	9
4.0	Electrical Design.....	15
5.0	Calibration	19
5.1	Static Calibration	19
5.2	Dynamic Calibration.....	22
6.0	Error Analysis.....	29
7.0	Exploding Foil Gun	34
8.0	Operating Instructions	41
9.0	Conclusions	43
10.0	Recommendations	44
	Appendix	

ILLUSTRATIONS

Figure 1	Beam Fixed at Both Ends - Concentrated Load at Midspan	6
2	Outline Drawing, Final Table Design	7
3	Photograph Thrust Table with Control Panel	8
4a	Outline Drawing, Multiplate Target (Target Chamber).....	12
4b	Outline Drawing, Multiplate Target (Spacer).....	11
4c	Outline Drawing, Multiplate Target (Retainer Ring)	12
5a	Impacted Target Plate	13
5b	Impacted Target Plate	14
6	Wheatstone Bridge.....	16
7	Strain Gage Placement	17
8	Bridge Circuit Diagram	18
9	Static Calibration Setup	20
10	Percent Elastic Potential Energy versus Gravitational Potential Energy	21
11	.22 Caliber Light Gas Gun	23
12	0.159 cm Diameter Projectile and .22 Caliber Sabot	24
13	Block Diagram of Kerr Cell Station	25
14	Shadowgraph of 0.159 cm Diameter Projectile	26
15	Baseplate Suspension System	28
16	Sanborn Recording of Bridge Output Voltage, Shot No. 1 ..	32
17	Measured Mass versus Shot Number.....	33
18	Exploding Foil Gun Facility	35

ILLUSTRATIONS (Concl'd)

Figure 19	Double Pulse Kerr Cell Shadowgraph	36
20	Impact Plate	37
21	Sanborn Recording of Exploding Foil Gun Shot	38
22	Exploding Foil Gun	40

TABLES

Table I	Light Gas Gun Calibration Shots	47
II	Gravitational Potential Energy	47
III	Thrust Table Mass	48

LABORATORY DATA SHEETS

1 - 2	Static Calibration, k_1	45
2 - 2	Static Calibration, k_2	46

LIST OF SYMBOLS

b	Beam width (m)
d	Beam thickness (m)
e_o	Output voltage (volts)
E	Modulus of elasticity (N/m^2)
I	Moment of inertia (m^4)
k	Spring constant (N/m)
k_1	Bridge sensitivity (volt/m)
k_2	Spring constant (N/m)
K_b	Kinetic energy of blow-off (Joules)
K_e	Elastic potential energy (Joules)
KE	Kinetic energy (Joules)
K_g	Gravitational potential energy of table top (Joules)
K_r	Rotational kinetic energy of thrust table (Joules)
K_w	Kinetic energy of base plate (Joules)
l	Length (m)
m	Mass (kg)
m_1	Mass of projectile (kg)
m_2	Mass of thrust table (kg)
n	Number of variates
R	Resistance (ohms)
V	Supply voltage (volts)
v_1	Velocity (m/s)

LIST OF SYMBOLS (Concl'd)

v_2	Velocity of thrust table (m/s)
w	Force (N)
x	Table motion in horizontal plane (m)
y	Deflection in the verticle plane (m)
Z_i	Variate deviation

A SYSTEM TO MEASURE THE MASS OF A PROJECTILE LAUNCHED FROM AN EXPLODING FOIL GUN

by
J. A. Morreal

1.0 SUMMARY

The momentum transfer from a projectile of unknown mass is measured with a modified ballistic pendulum in the form of an inverted thrust table. Kinetic energy of the table after impact is stored as elastic potential energy in the spring system of the thrust table. The distance the table moves is measured with a strain gage bridge attached to the flat spring flexures. Using the known constants of table mass, and spring constant the momentum transfer is calculated. If the projectile velocity is known, then the projectile mass can be calculated.

Dynamic calibration of the thrust table was obtained by impacting the target attached to the table with projectiles of known mass and known velocities. The Avco light gas gun was used to launch projectiles of 5.8 mg with velocities of from 6 to 7.5 km/s.

Ten calibration shots were made. Data spread about the mean value was $\pm 5\%$.

The calorimetric method of measuring the kinetic energy of the projectile as a backup to the ballistic method was dropped early in the program due to experimental difficulties in minimizing heat loss.

2.0 INTRODUCTION

The probability of damage to spacecraft structures by micrometeorite impacts increases as the periods of flight are extended. Protection from this hazard is important particularly when manned spacecraft are considered. The design of armor to neutralize these impacts will require laboratory simulation of some kind. The launching of projectiles of known velocity up to 7.5 km/s and shape is an accomplished fact using light gas gun launchers. Since the shape of the projectile is preserved, the mass of the impacting particle is known.

Exploding foil guns are currently being investigated as a means of launching flat mylar plates of approximately 10 mg mass at velocities above 7.5 km/s. The difficulty with the exploding foil gun is that the projectile shape is not preserved during launch and most likely changes during flight. The mass is therefore unknown and a means must be provided to measure it at impact.

To accomplish the mass measurement, two techniques were initially considered. A calorimeter was proposed to measure the kinetic energy of the projectile and a ballistic pendulum was proposed to measure the momentum transfer. Experimental results showed early in the program that large heat losses and difficulty in controlling them made the calorimeter approach impractical.

An inverted thrust table using flat spring flexures was proposed as a practical extension of the simple pendulum for the measurement of the momentum transfer. The thrust table's relative compactness, large dynamic range, ease of electrical readout and ruggedness made it an attractive substitute for the simple pendulum.

3.0 THEORETICAL CONSIDERATIONS

In the case of the inverted thrust table, the momentum transfer imparts to the thrust table a certain amount of kinetic energy which is transferred to the compressed spring rather than going into gravitational potential energy as is the case of the simple pendulum.

Since momentum is conserved, one can write

$$m_1 v_1 = m_2 v_2 \quad (1)$$

Immediately after impact, the table will have a certain kinetic energy as a result of its motion and if the projectile is completely captured by the target the following expression can be written:

$$KE = \frac{1}{2} (m_1 + m_2) v_2^2 \quad (2)$$

If $m_2 \gg m_1$, equation (2) can be written with very small error.

$$KE = \frac{1}{2} m_2 v_2^2 \quad (3)$$

Since the kinetic energy is used to compress the spring system, one can write

$$\frac{1}{2} m_2 v_2^2 = \int_0^x k x dx \quad (4)$$

where k is the spring constant in N/m and x is the distance the springs are compressed in m. Performing the integration in equation (4),

$$\frac{1}{2} m_2 v_2^2 = \frac{k x^2}{2} \quad (5)$$

and solving for v_2 ,

$$v_2 = \left(\frac{k x^2}{m_2} \right)^{1/2} \quad (6)$$

Substituting this value of v_2 in equation (1) and solving for m_1 ,

$$m_1 = \frac{m_2}{v_1} \left(\frac{k x^2}{m_2} \right)^{1/2} = \frac{m_2^{1/2} k^{1/2} x}{v_1} \quad (7)$$

Equation (7) is the basic equation for calculating the mass, m_1 , if its velocity is known. The mass, m_2 , can be measured with a balance and the spring constant is determined statically. The distance x is measured electrically by use of strain gages attached to the springs flexures.

Equation (7) should include two other terms, one to account for rotational kinetic energy, if there is any, and one to account for the gravitational potential energy since the table moves up a small amount as well as horizontally.

Rewriting (5) to account for these effects

$$\frac{1}{2} m_2 v_2^2 = \frac{kx^2}{2} + K_g + K_r \quad (8)$$

Solving for v_2 and substituting in equation (1),

$$m_1 = \frac{m_2^{1/2}}{v_1} [kx^2 + 2(K_g + K_r)]^{1/2} \quad (9)$$

It was assumed in equation (1) that there was a perfectly inelastic collision. This is not true and considerable time was expended in arriving at a suitable target that would capture the projectile and minimize the effects of high-energy impacts. Ejecta and vaporized material from impacts into open-cone type targets produced mass readings of up to 50% above that of the known projectile mass because of the reaction from the high velocity blowoff. Blowoff errors will be a function of the velocity and material of the projectile. Thickness and hardness of the target impact plates will have to be matched to the set of conditions that prevail. A measurement of the blowoff mass was not possible in the time available during the development of this instrument. The error due to blowoff was assumed to be that which remained after all other sources of error were accounted for. Equation (9) is modified to include the effect of blowoff.

$$m_1 = \frac{m_2^{1/2}}{v_1} [kx^2 + 2(K_g + K_r - K_b)]^{1/2} \quad (10)$$

3.1 Mechanical Design of Thrust Table

Using formula (7), a mass for the table is chosen and by arbitrarily limiting the travel to one centimeter, a spring constant can be calculated for a given momentum. The maximum momentum is obtained when

$$m_1 = 30 \text{ mg} \quad \text{and} \quad v_1 = 15 \text{ km/s}$$

let $m_2 = 1 \text{ kg}$

then

$$k = \frac{m_1^2 v_1^2}{m_2 x^2} = \frac{9 \times 10^{-4} \times 2.25 \times 10^{12}}{10^3 \times 1^2} = 2.03 \times 10^3 \text{ N/m}$$

For a deflection of 1 cm the force is therefore 20.3 Newtons.

A close approximation for the elastic curve equation for the flat springs is given by

$$y = \frac{1}{48} \frac{W}{EI} (3lx^2 - 4x^3)$$

This is the elastic curve equation from A to B for a beam fixed at both ends and a concentrated load at the center as shown in figure 1. The maximum deflection, y , at b is

$$y = - \frac{1}{192} \left(\frac{W l^3}{EI} \right) \quad (11)$$

Nicholson ground flat stock 0.795 mm (1/32 inch) thick by 25.4 mm (1 inch) wide was chosen as the spring material. A length is calculated for a deflection of 1 cm with a given force of $\frac{20.3}{4} = 5$ Newtons. The moment of inertia of the cross section is calculated from

$$I = \frac{b d^3}{12} \text{ cm}^4 = 1.06 \times 10^{-12} \text{ m}^4 \quad (12)$$

The modulus of elasticity of steel is taken as

$$E = 3 \times 10^7 \frac{\text{lb}}{\text{in}^2} = 2.07 \times 10^{11} \frac{\text{N}}{\text{m}^2}$$

Solving equation (11) for l and evaluating,

$$l = \left(\frac{192 y EI}{W} \right)^{1/3} = 0.43 \text{ m} \quad (13)$$

3.2 Final Mechanical Design

The final design has the dimensions shown in figure 2. Figure 3 is a photograph of the thrust table and control panel. The flat spring flexures are

UNCLASSIFIED

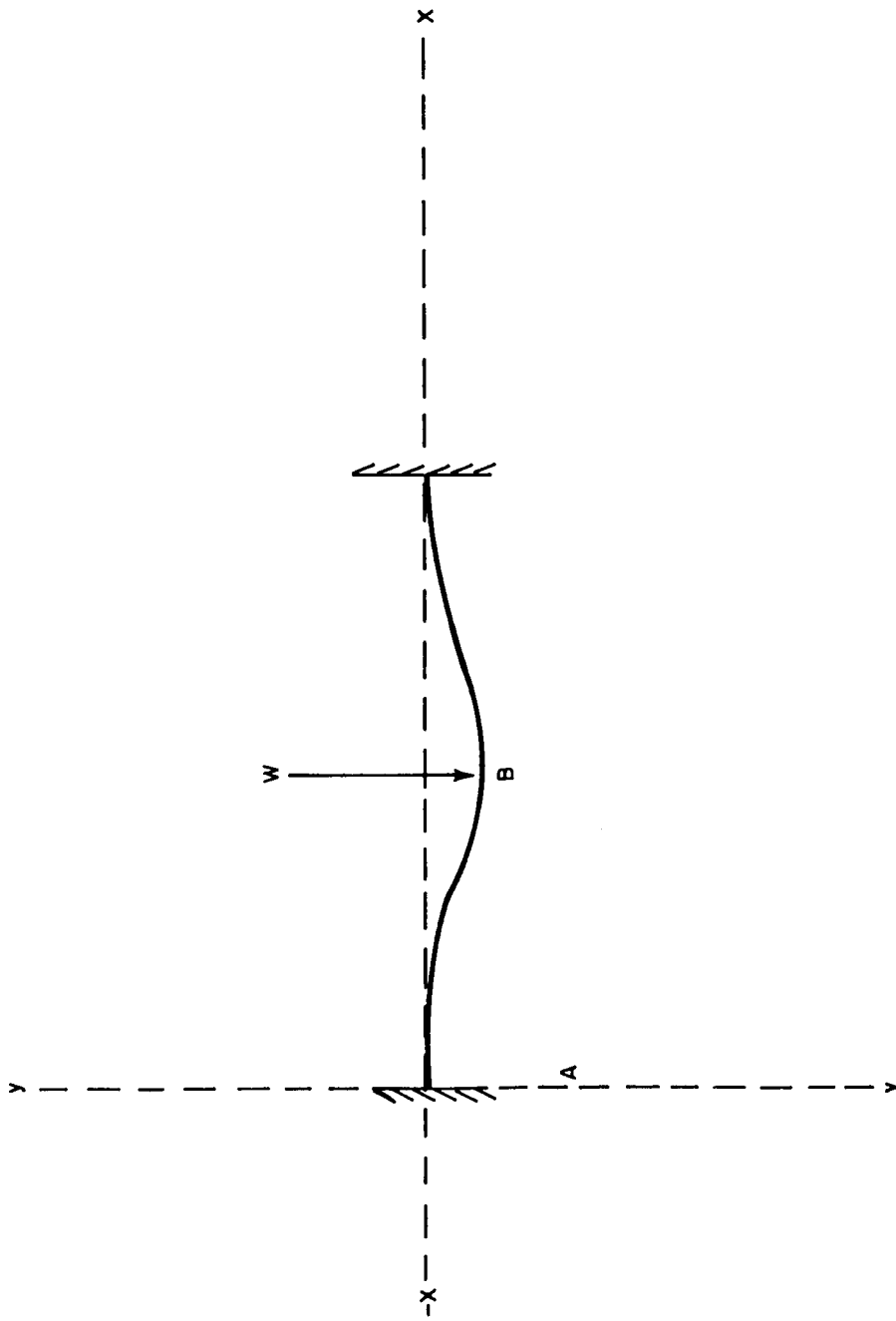
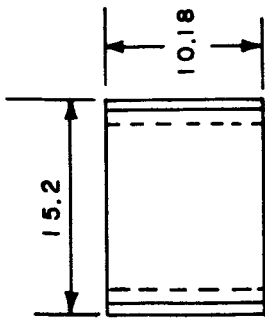


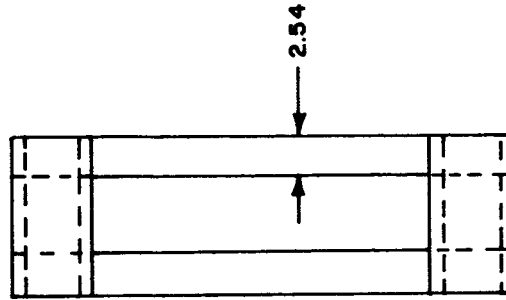
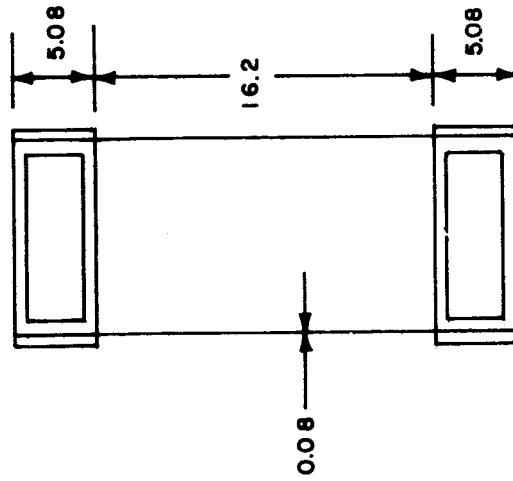
Figure 1 BEAM FIXED AT BOTH ENDS - CONCENTRATED LOAD AT MIDSPAN

86-5280

UNCLASSIFIED

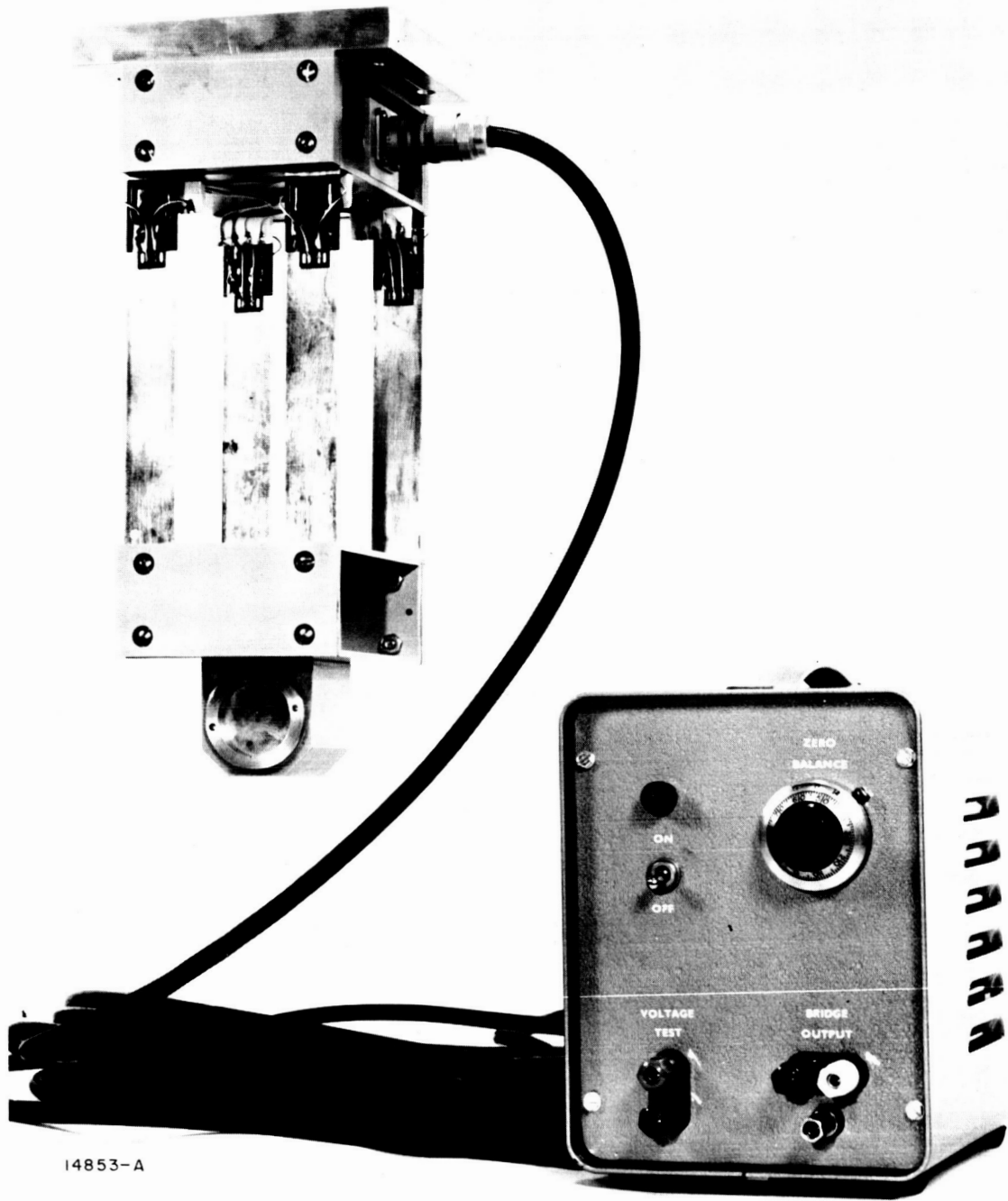


NOTE: ALL DIMENSIONS ARE
IN CENTIMETERS



86-8462

Figure 2 OUTLINE DRAWING, FINAL TABLE DESIGN



14853-A

Figure 3 PHOTOGRAPH THRUST TABLE WITH CONTROL PANEL

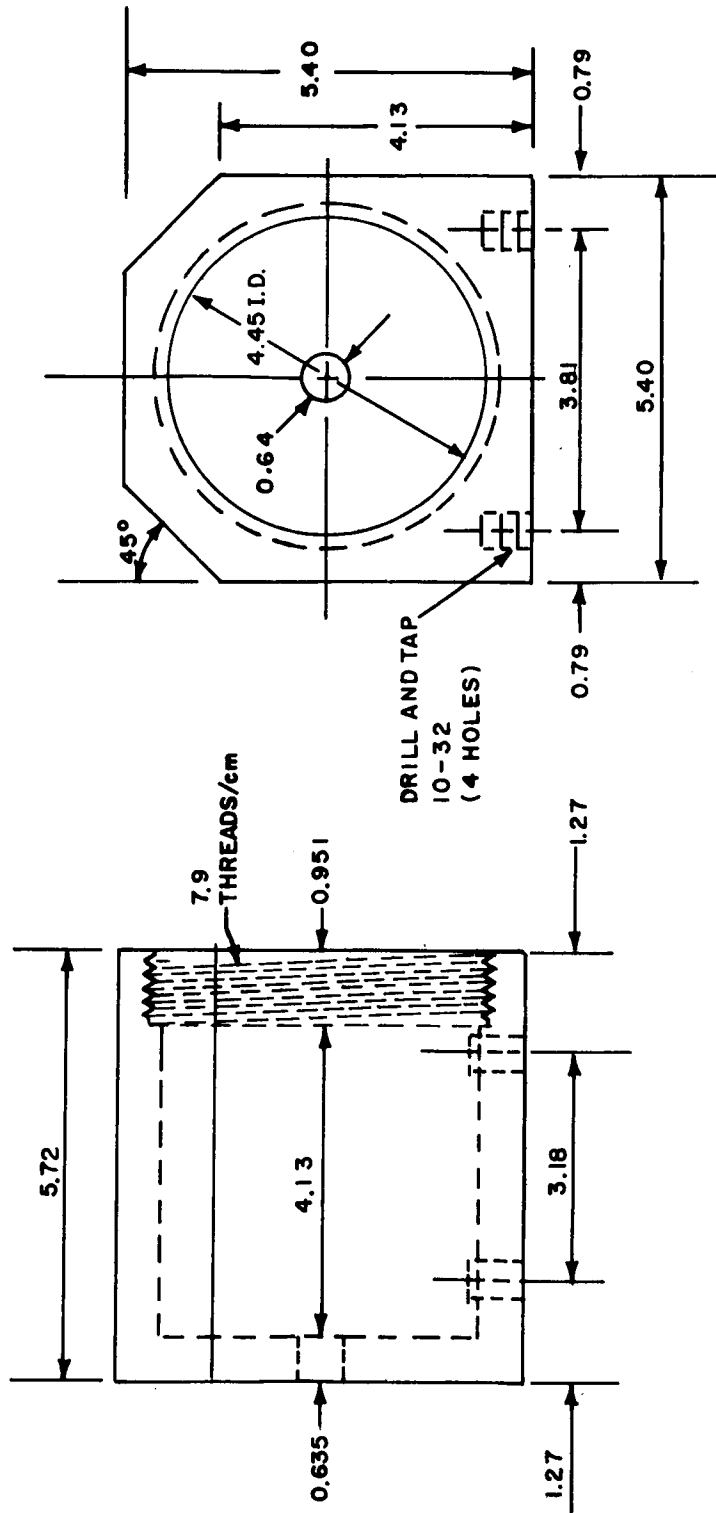
Nicholson ground flat stock 0.079 cm ($\frac{1}{32}$ inch) thick by 2.54 cm (1 inch) wide hardened to Rockwell C. 63-65. The end clamps and base are aluminum. Table III lists the mass of each part and the total mass for the table top is calculated. The mass of the spring flexures is approximated by the formula $m = \frac{33}{140} m_2 l$ where m_2 is the mass per unit length and l is the length of the spring. This value is that used for vibrational loading of a cantilever and is considered a close approximation.

3.3 Multiplate Target

A multiplate target similar to that shown in figure 4 was designed to minimize the effect of blowoff. Venting of the rear of the target partially neutralizes the effect of escaping vapors through the impact hole in the first plate. For these tests the plates used were 0.127-mm thick, soft copper spaced 6.4 mm apart. The target is constructed so that up to 7 plates can be used. Figures 5a and 5b show a typical set of plates impacted with a 5.8 mg ball with a velocity of 6.3×10^5 km/s.

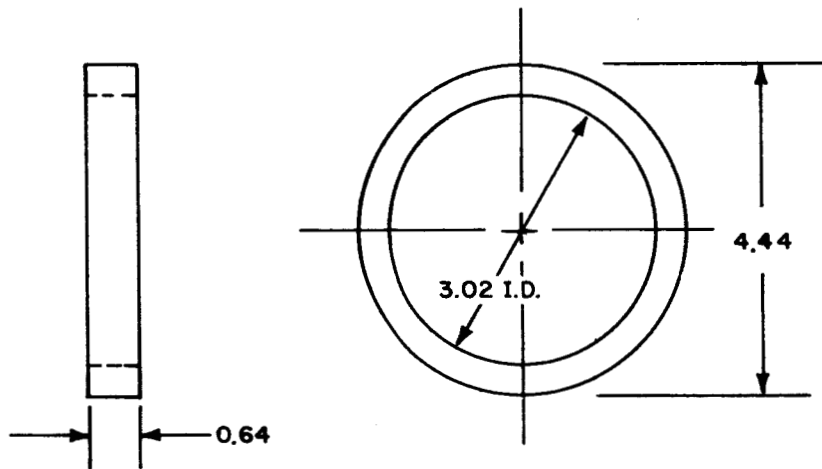
The target is prepared for a shot by alternately loading impact plates and spacers in the target chamber. Each plate is pierced with a small hole so that the target chamber obtains ambient pressure when placed in the range vacuum.

NOTE: ALL DIMENSIONS
ARE IN CENTIMETERS



86-8463

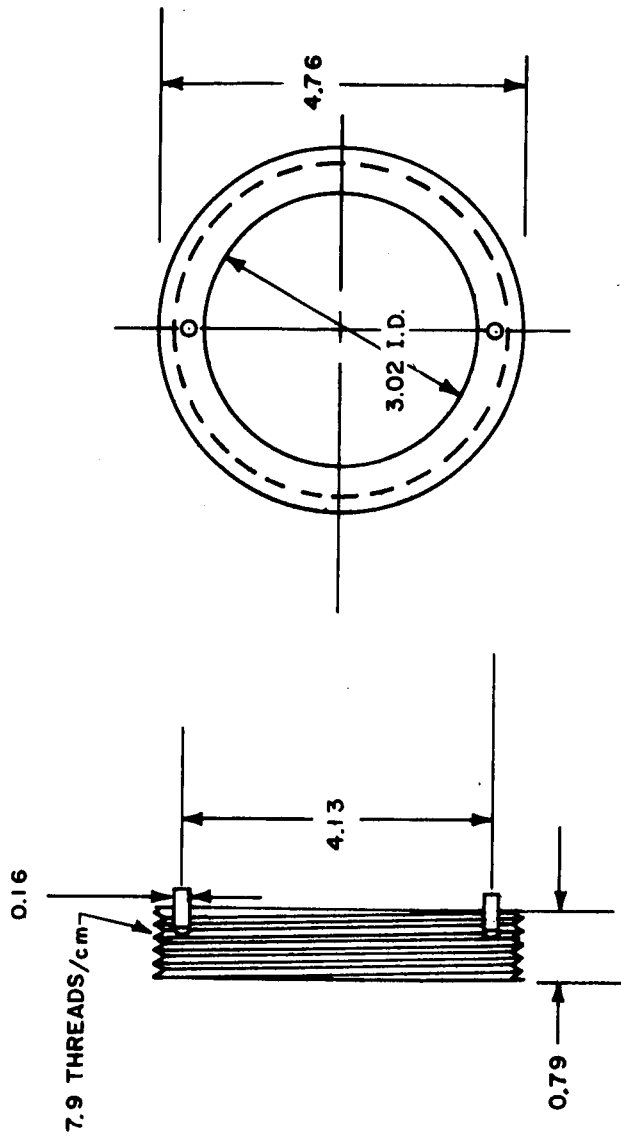
Figure 4a OUTLINE DRAWING, MULTIPLATE TARGET (TARGET CHAMBER)



86-8464

NOTE: ALL DIMENSIONS ARE
IN CENTIMETERS

Figure 4b OUTLINE DRAWING, MULTIPLATE TARGET (SPACER)



NOTE: ALL DIMENSIONS
ARE IN CENTIMETERS

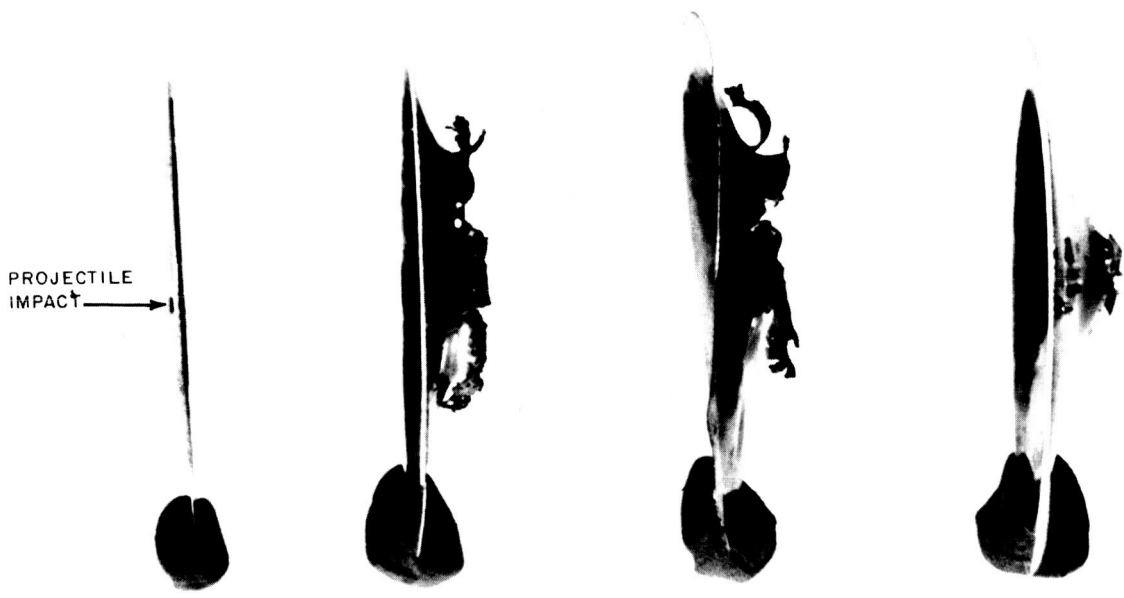
86-8465

Figure 4c OUTLINE DRAWING, MULTIPLATE TARGET (RETAINER RING)



14837B

Figure 5a IMPACTED TARGET PLATE



14837A

Figure 5b IMPACTED TARGET PLATE

4.0 ELECTRICAL DESIGN

The Wheatstone bridge circuit shown in figure 6 is used to measure the small resistance changes in the strain gages when they are activated. The applied dc voltage, E , is supplied by a well regulated transistorized power supply. The output voltage of the bridge is monitored with a suitable meter having a resistance represented by R_m .

A symmetrical, four-active-arm bridge is used with arms 1 and 4 in tension and 2 and 3 in compression. Nominally $R_1 = R_2 = R_3 = R_4 = R_o$. Under these conditions, the output voltage, e_o , is obtained from the following equation:

$$e_o = \frac{\Delta R V}{R_o} \quad (14)$$

Where ΔR is the change in resistance of one gage. A more accurate expression would include the meter resistance, R_m , so that

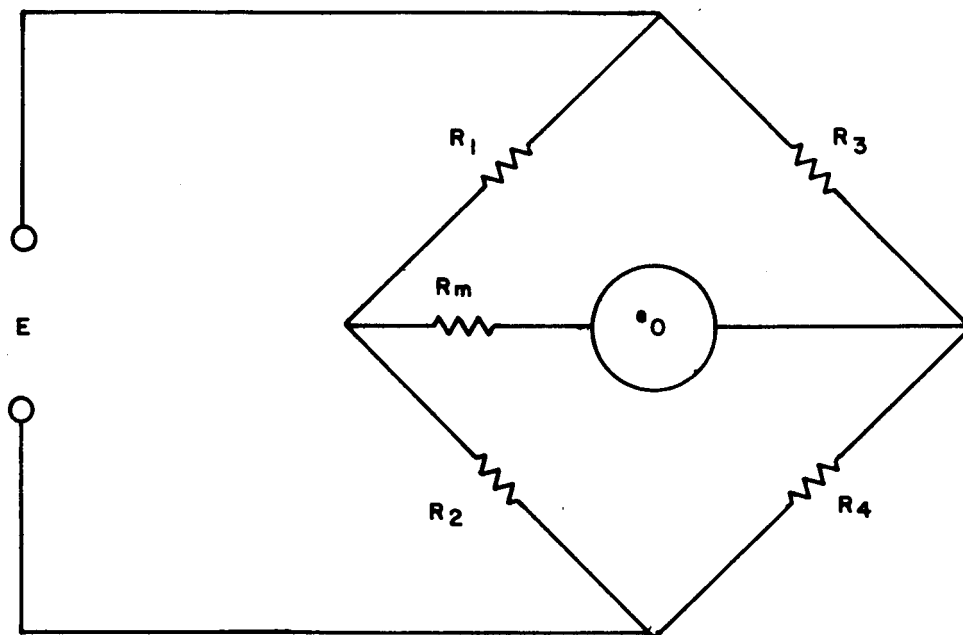
$$e_o = V \frac{\Delta R/R_o}{1 + \left(\frac{R_o}{R_m}\right) \left[1 - \left(\frac{\Delta R}{R_o}\right)^2\right]} \quad (15)$$

If $\frac{R_o}{R_m} \ll 1$, then the expression reduces to equation (14) which is completely

linear. What this all means is that if the meter resistance, or any device which is used for readout, has a high input impedance compared to the bridge output resistance (4K), then nonlinearity of the bridge circuit would not be a problem. A Sanborn recorder with an AC-DC plugin (4 megohms) or a Tektronix oscilloscope with a preamplifier of one megohm input impedance are typical instruments which can be used for the readout meter.

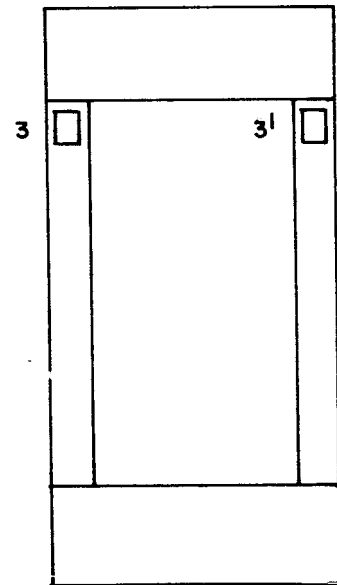
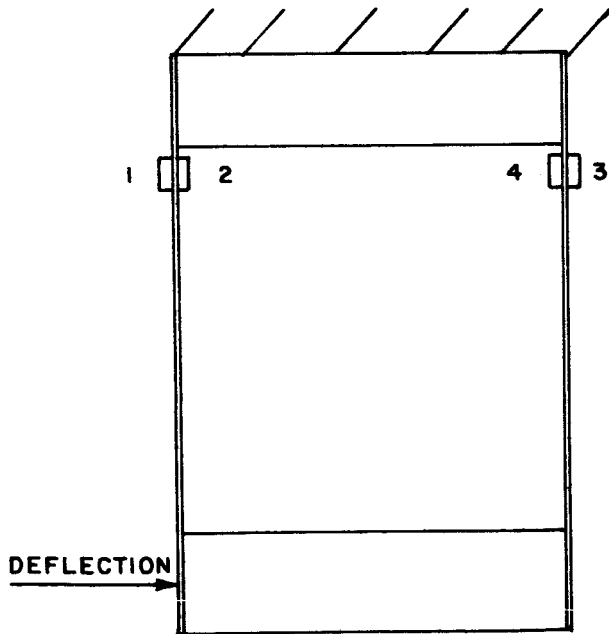
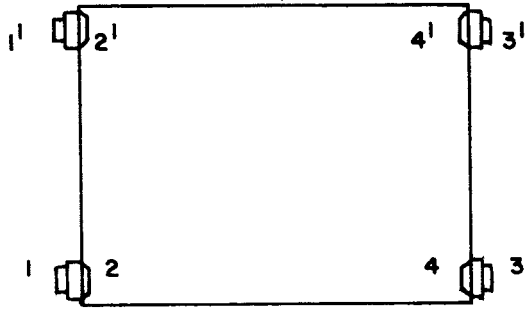
The power supply that is used is completely floating so that single-ended readout can be used if necessary. However, better isolation from noise pick-up, particularly in the exploding foil gun facility, is obtained when a balanced output is used.

In order to obtain maximum sensitivity, a double bridge is used. The physical placement of the gages is shown in figure 7. The circuit diagram of the complete system is shown in figure 8. The strain gages used are SR-4 type C-14 with a resistance of 2000 ohms. Resistances R_1 , R_2 , R_3 , and R_4 comprise the bridge zero balance network.



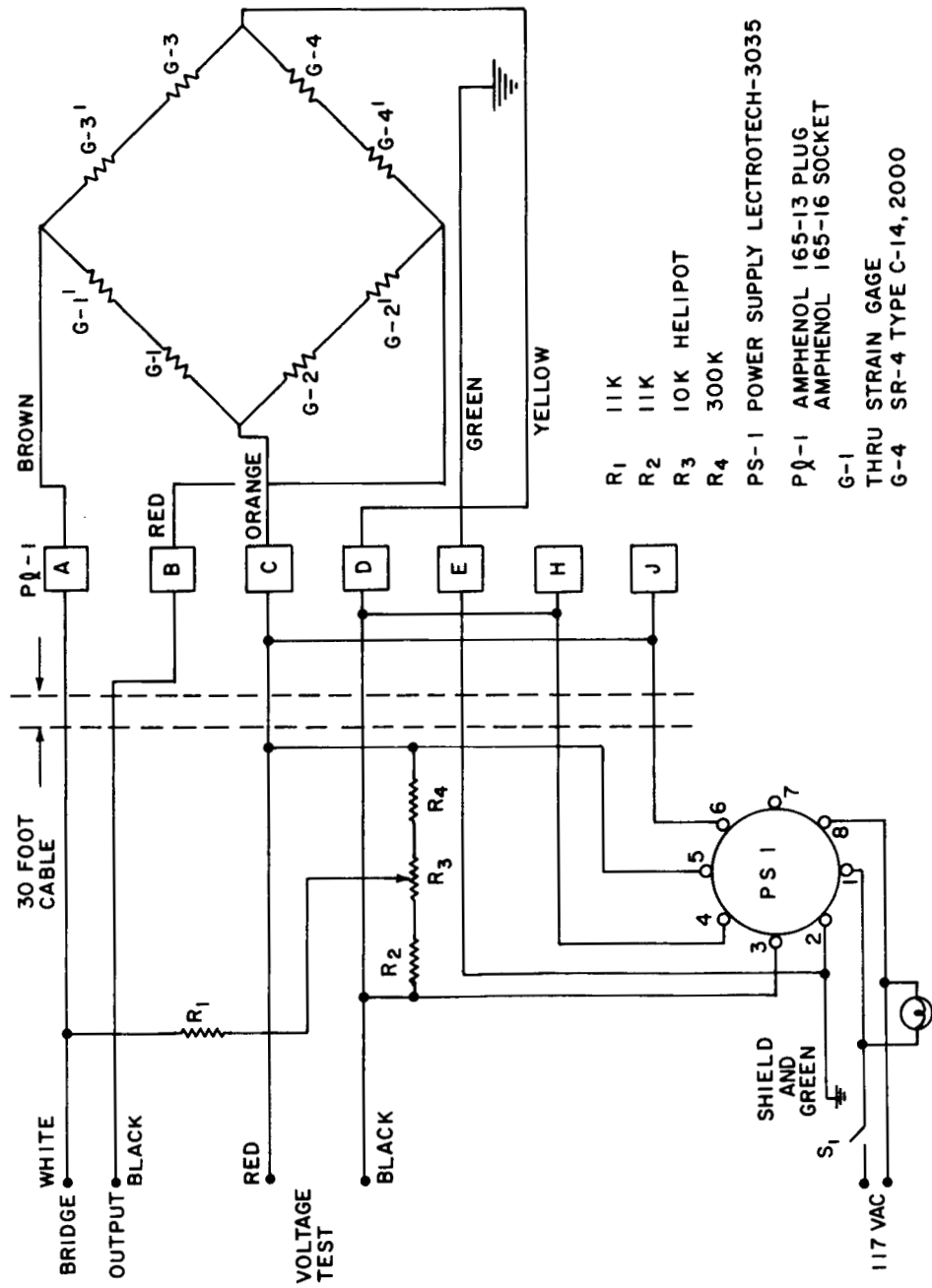
86-5282

Figure 6 WHEATSTONE BRIDGE



86-5283

Figure 7 STRAIN GAGE PLACEMENT



86-5278

Figure 8 BRIDGE CIRCUIT DIAGRAM

5.0 CALIBRATION

5.1 Static Calibration

The bridge sensitivity, k_1 , was determined by measuring the output voltage as the table was moved fixed known amounts. In order to accomplish this, the table base was fixed to a rigid structure to which a micrometer was also attached. (See figure 9). Output voltage was measured with a differential voltmeter. The results are listed in laboratory data sheet number 1-2. The bridge sensitivity thus determined is $k_1 = 9.17$ v/m. The spring constant, k_2 , in Newtons/volt was then measured using the same physical arrangement except a spring scale was used to deflect the table. The output voltage for full scale deflection is tabulated on laboratory data sheet number 2-2. The value of k_2 thus determined is $k_2 = 2.32 \times 10^2$ N/v.

The spring constant, k , in dynes/cm is obtained by combining k_1 and k_2 .

$$k = k_1 k_2 = 2.12 \times 10^3 \text{ N/m}$$

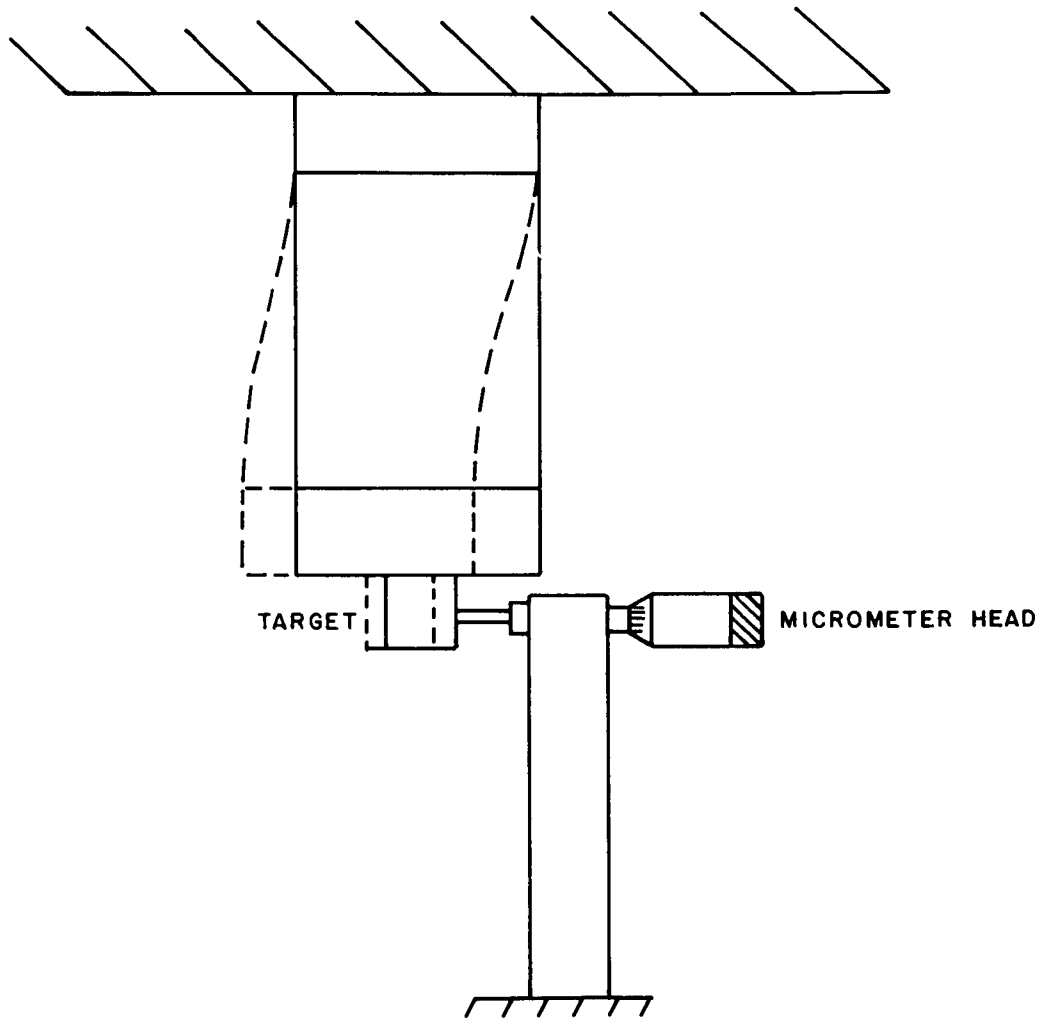
In order to determine if off-center impacts would affect the bridge sensitivity, static deflections of the thrust table were made with the point of contact made in all four quadrants 2.5 cm from the center of the target. No change in bridge sensitivity was detected.

The gravitational potential energy of the table was determined by statically measuring the change in height for given horizontal deflections with the result shown in table II. For these same horizontal deflections the elastic potential

energy is calculated from $K_e = \frac{kx^2}{2}$ where x is the horizontal deflection and k the

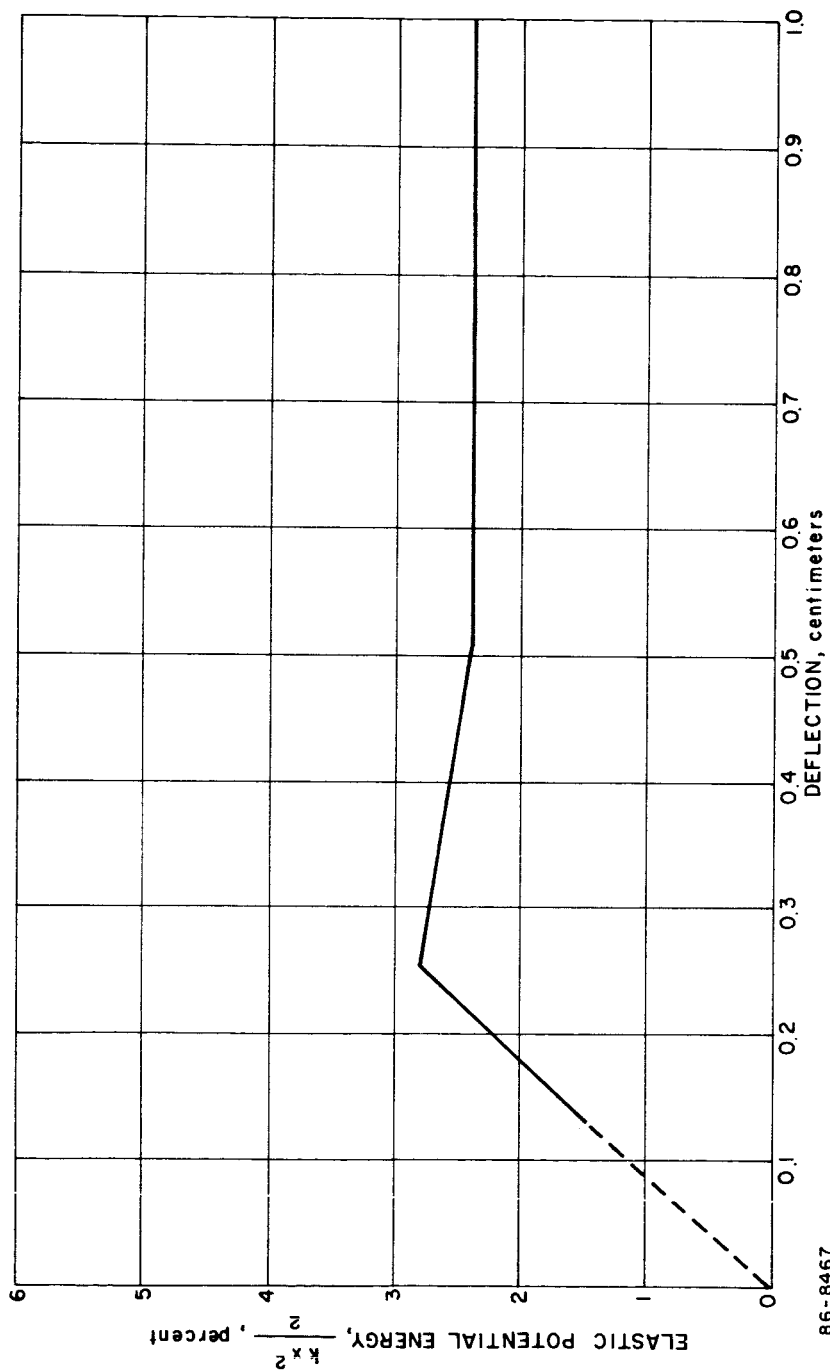
spring constant. From this the percentage of gravitational energy is calculated and the results are plotted in figure 10 as a function of horizontal displacement. At deflections less than 0.127 cm, this correction is approximately 1%. When reducing the experimental data, therefore, the procedure is to first calculate the horizontal displacement of the table from the bridge output voltage and the known bridge sensitivity, k_1 . The elastic potential energy which is stored in the compressed springs of the thrust table is then calculated from the measured value of x and the constant, k . The gravitational potential energy is determined by taking the appropriate percentage of the elastic potential energy corresponding to the horizontal deflection x , as indicated in figure 10.

The rotation of the table at a static deflection of 10.2 cm was less than the resolution of the measuring system. At time, $t = 37$ msec, w is therefore less



86-8466

Figure 9 STATIC CALIBRATION SETUP



86-8467

Figure 10 PERCENT ELASTIC POTENTIAL ENERGY VERSUS GRAVITATIONAL POTENTIAL ENERGY

than 8×10^{-3} rad/sec. The rotational kinetic energy $KE = 1/2 I \omega^2$ is therefore less than 2.03×10^{-11} N and can be ignored. Equation (10) can therefore be written as

$$m_1 = \frac{m_2^{1/2}}{v_1} [kx^2 + 2(K_g - K_b)]^{1/2} \quad (16)$$

5.2 Calibration-Dynamic

The thrust table was dynamically calibrated by launching 5.80 mg projectiles into the target at known velocities. Figure 11 is a photograph of the Avco .22 caliber light gas gun facility used to launch the projectile. The blast tanks remove most of the gun gases and a one mil- (.0254 mm) thick mylar diaphragm placed in the range pipe between the range pipe and the target tank removed any small amount of debris that followed the projectile.

A sabot was used to launch the projectile so that the mass of the projectile would be preserved. Figure 12 shows the cross section of the sabot with the 1/16"-(1.59 mm) diameter ball projectile in place.

The velocity of the projectile is measured by recording the time that the projectile traverses a known distance. Photographic recording stations are used to obtain maximum accuracy of the velocity measurement in the following way: A fiducial wire is placed in the field of each photographic station. Precise measurements of distance between wires are made and the optical axis of the station is accurately placed perpendicular to the trajectory. An electronic counter is used to measure the elapsed time. Start and stop triggering pulses for the electronic counter are produced by the photographic stations at the instant each picture is taken. A means is provided to trigger the photographic station when the projectile is in the vicinity of each fiducial wire. A block diagram of a photographic recording station is shown in figure 13.

The photographic recorder is a spark shadowgraph system with a 0.076 m field and shuttered by means of an electro-optical Kerr cell shutter. Figure 14 is a shadowgraph picture taken during shot No. 1 which demonstrates the ability of the system to verify the integrity of the projectile as well as providing a means of accurately measuring the velocity.

Vibrations generated by the launching of the projectile caused considerable difficulty in making the mass measurement. These vibrations apparently travel through the gun structure and the floor and arrive at the target tank at approximately the same time as the projectile. A noise pulse is therefore generated in the thrust table at the same time as the impact pulse. Isolating the range

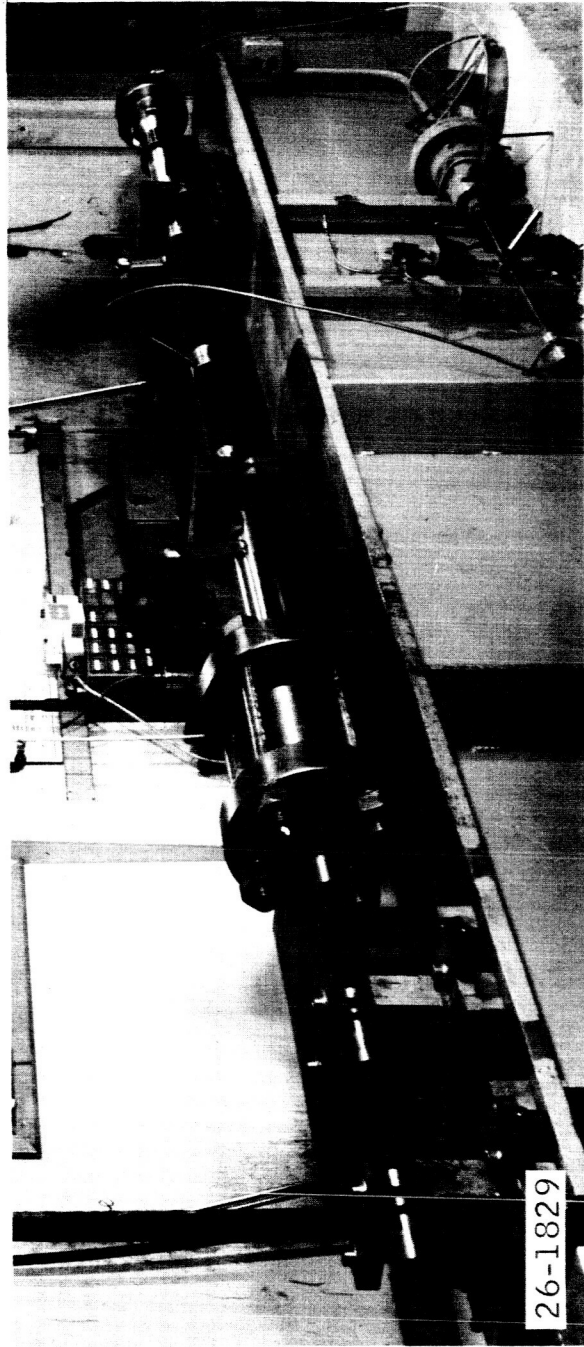


Figure 11 .22 CALIBER LIGHT GAS GUN

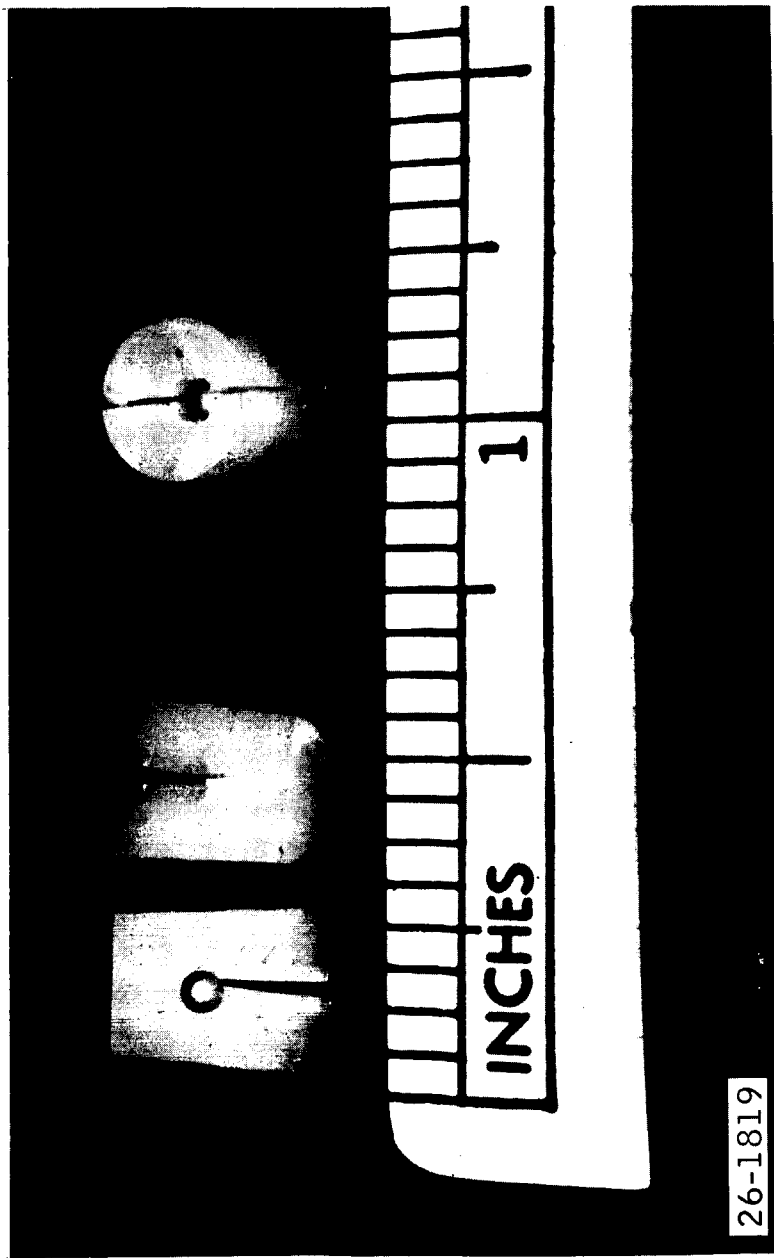
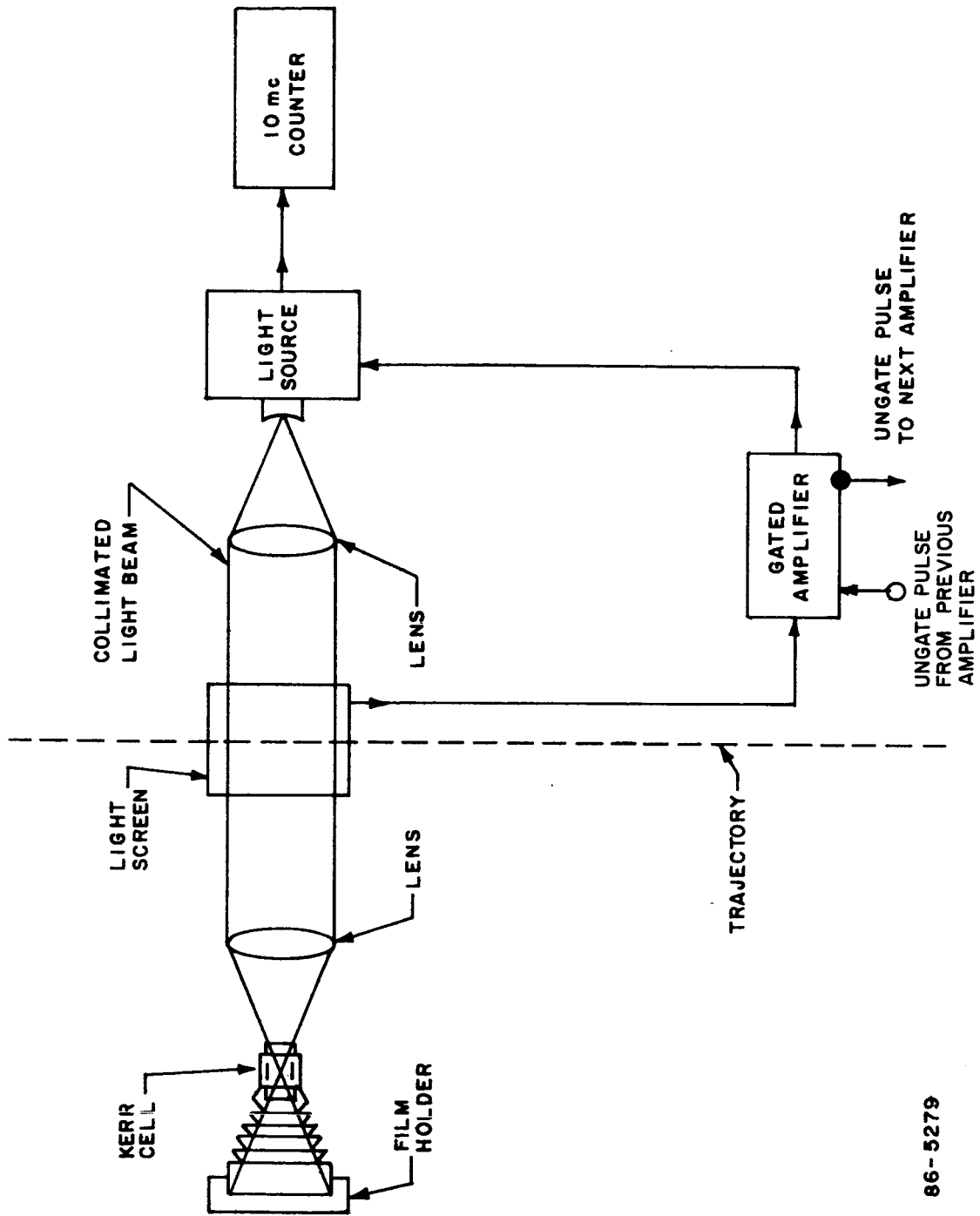


Figure 12 0.159 cm DIAMETER PROJECTILE AND .22 CALIBER SABOT



86-5279

Figure 13 BLOCK DIAGRAM OF KERR CELL STATION

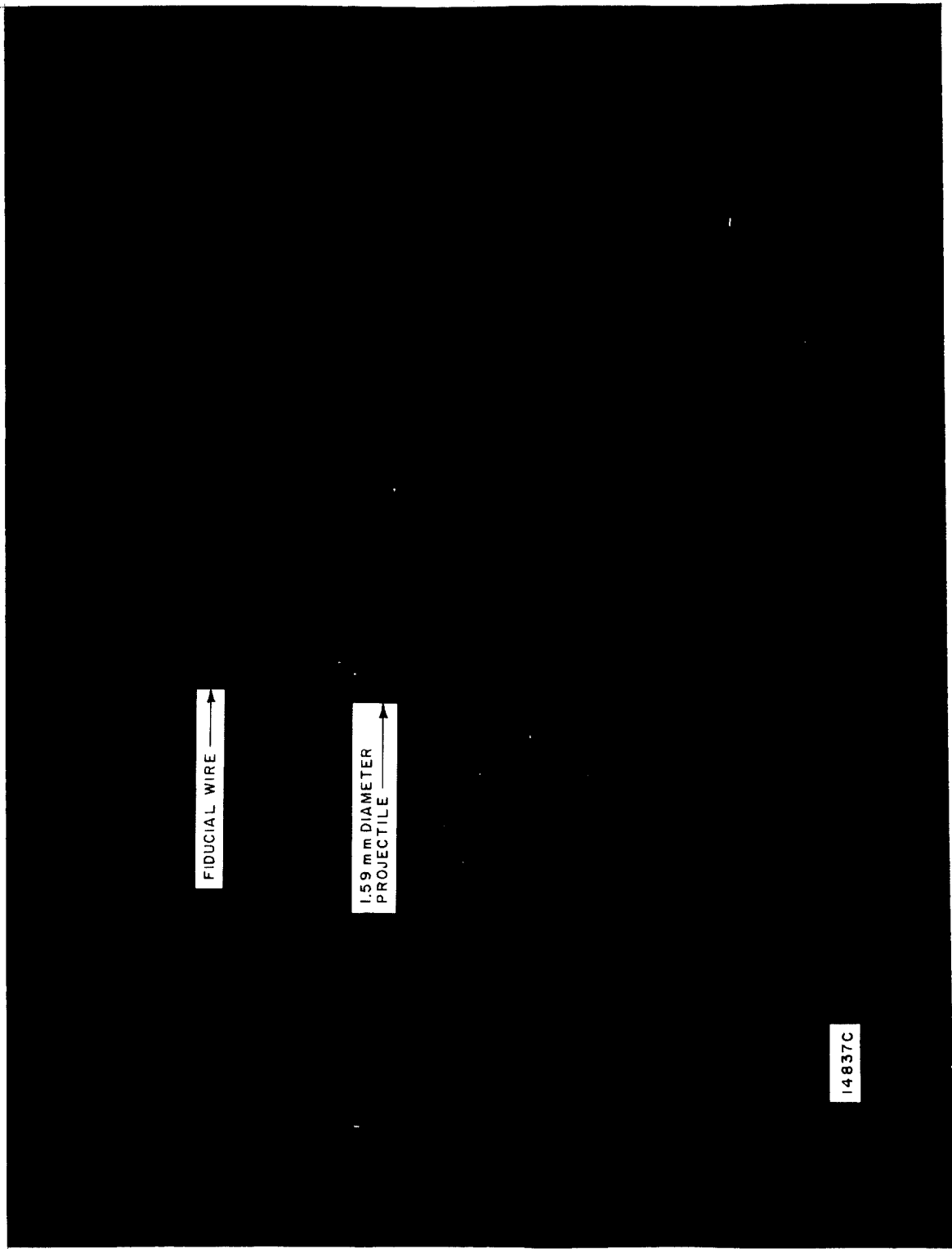


Figure 14 SHADOWGRAPH OF 0.159 cm DIAMETER PROJECTILE

pipe from the target tank did not reduce the noise pulse significantly. The final solution to the problem was to suspend the thrust table from a massive base plate which was in turn suspended from the top of the target tank with long limber springs. The base plate was loaded with lead blocks until its natural frequency was approximately 1 Hz. Figure 15 is a drawing of the final system that was used during the calibration of the thrust table. A number of sabots was launched without projectiles to test the system for its vibration isolation abilities. No significant noise was detected.

In solving the vibration problem, however, another problem was generated. Reaction of the base plate to the impact of the thrust table represents an energy loss that must be accounted for. Attempts to measure the motion of the base plate directly were foiled by the noise level in the range facility. It was decided to analyze the system mathematically and compute the motion of the base plate during the time it takes the thrust table to reach its first peak.

The Appendix is a discussion of the method used in analyzing the complete dynamic system used in the calibration of the thrust table on the .22 calibre light gas gun range.

The computer analysis shows that for the average test conditions obtained on the .22 calibre light gas gun range, the base plate will have a kinetic energy of approximately 7×10^{-6} N or 1.4% of the kinetic energy of the thrust table at 37 msec after impact.

The elastic potential energy that is stored in the spring system of the thrust table is therefore reduced by this amount. Equation (16) is accordingly modified for the purposes of reducing the ballistic range data to include the reaction of the base plate, K_w .

$$m_1 = \frac{m_2^{1/2}}{v_1} [kx^2 + 2(K_g + K_w - K_b)]^{1/2} \quad (17)$$

This equation is used only in reducing the data obtained in the light gas gun facility at Avco using the base plate suspension system for vibration isolation. In reducing data that is obtained from a light gas gun installation with no base plate suspension system, the term, K_w , is deleted from equation (17).

The rotational kinetic energy, K_r , is small enough to be ignored and is omitted.

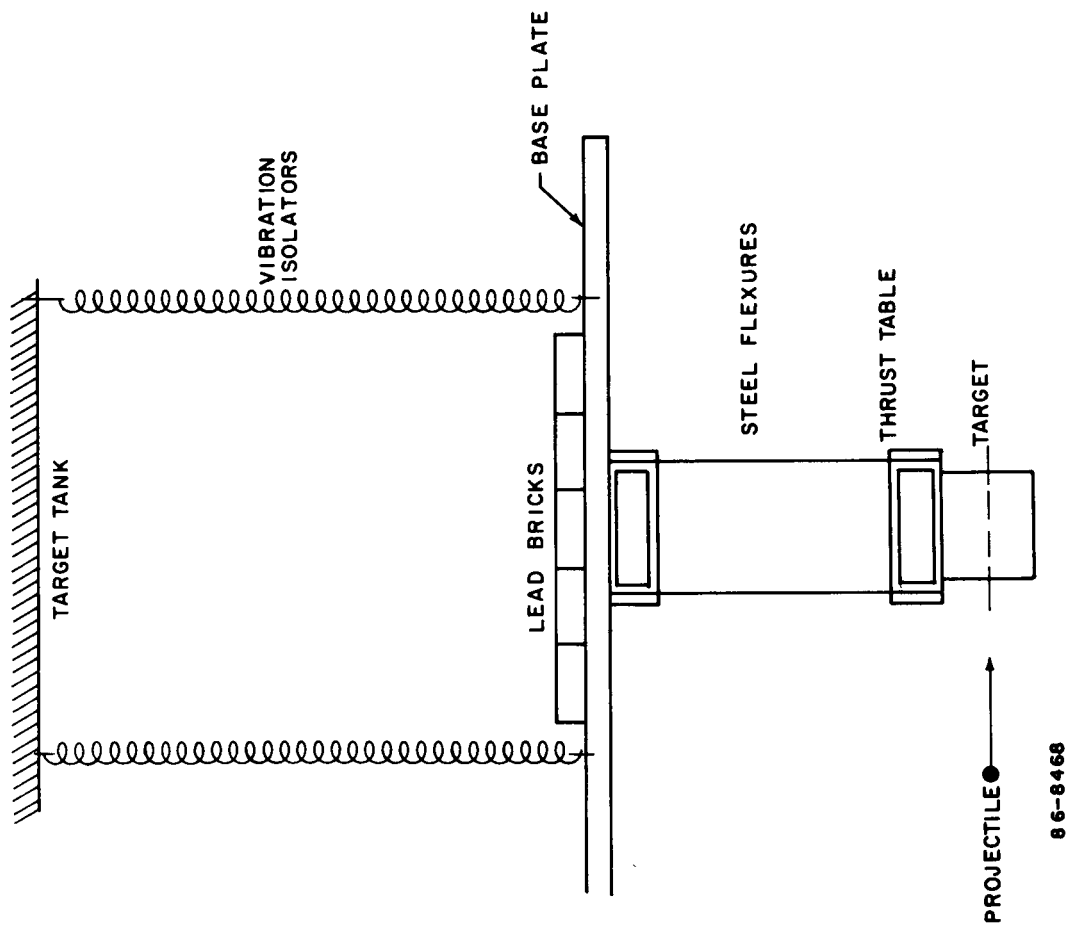
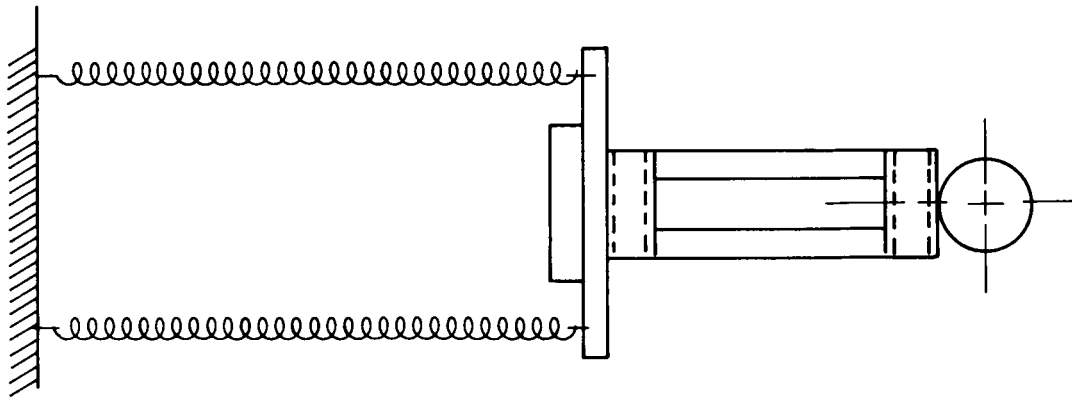


Figure 15 BASEPLATE SUSPENSION SYSTEM

6.0 ERROR ANALYSIS

The experimental and estimated errors of the various terms of equation (17) are determined and combined to establish the overall system accuracy.

The mass of the table, m_2 , was measured on a gram balance to an accuracy of 1 part in 9600. The error in this reading was considered small enough to be neglected.

The mean value for the bridge sensitivity, k_1 , was obtained from the 14 data points listed in Laboratory Data Sheet No. 1-1. The standard deviation was then determined using the formula

$$\sigma = \left(\frac{1}{n-1} \sum_{i=1}^n z_i^2 \right)^{1/2} \quad (18)$$

The value for k_1 established was

$$k_1 = 9.17 \pm 0.08 \text{ v/m}$$

In a similar manner using the data from Laboratory Data Sheet No. 1-2, the mean and standard deviation for k_2 is established.

$$k_2 = 2.32 \pm 0.09 \times 10^2 \frac{N}{V}$$

The spring constant is determined by combining k_1 and k_2

$$k = k_1 k_2$$

and the standard deviation is determined from the approximate formula

$$\sigma^2 \approx \left[\left(\frac{\partial k}{\partial k_1} \right) \sigma_{k_1} \right]^2 + \left[\left(\frac{\partial k}{\partial k_2} \right) \sigma_{k_2} \right]^2 \quad (19)$$

The value for k thus determined is

$$k = 2.12 \pm 0.08 \times 10^3 \frac{N}{m}$$

The standard deviation of x is determined from k_1 and the output voltage reading, e_o . A Sanborn recorder with zero suppression was used to obtain the output

voltage data during the dynamic calibration of the thrust table. The voltage is read to an accuracy of 1 part in 80. From the expression $x = \frac{e_o}{k_1}$, the standard deviation is obtained using the formula

$$\sigma_x^2 \approx \left[\left(\frac{\partial x}{\partial k_1} \right) \sigma_{k_1} \right]^2 + \left[\left(\frac{\partial x}{\partial e_o} \right) \sigma_{e_o} \right]^2 \quad (20)$$

A value for x and σ_x is established for conditions obtained when $m_1 = 5.8 \times 10^{-3}$ Kg and $v_1 = 6 \times 10^3$ m/s

$$\sigma_x = 0.14 \text{ mm}$$

$$x = 0.874 \pm 0.014 \text{ mm}$$

The value of σ_x will depend upon the accuracy of the instrumentation used to record e_o and will have to be recalculated each time the instrumentation is changed.

In measuring the projectile velocity, measurements of time and distance were made using techniques previously discussed. The distance was 61 cm and measured to an accuracy of $\pm 1.27 \times 10^{-5}$ m. At velocity of 6×10^3 m/s, the time was measured to an accuracy of 1 part in 1000. The velocity error is 0.1% and is considered small enough to be neglected. It should be noted that this measurement is of the average velocity over the distance between light stations and the velocity measuring station is approximately 2 meters from the target. It is assumed that the drag on the projectile at the range pressures used would be negligible.

The gravitational potential energy was determined by measuring the vertical displacement with a dial indicator while the table was deflected fixed known amounts horizontally. Table II lists the value for the gravitational potential energy and the measurement error at five horizontal deflections. The minimum displacement that could be measured directly was $0.254 \mu\text{m}$ which corresponds to a horizontal deflection of 1.27 mm. At a horizontal deflection of 0.874 mm which corresponds to the test conditions for the light gas gun shots, the vertical displacement is estimated to be $1.27 \pm 1.27 \mu\text{m}$. The gravitational potential energy is therefore $K_g = (980)(962)(1.27) \pm 1.27 \times 10^{-4} = 120 \pm 120 \times 10^{-7}$ Joules.

The estimated error in the computed value for the kinetic energy of the base plate using the digital computer is $\pm 10\%$.

The blowoff error is unknown and is estimated from the experimental results obtained in the light gas gun shots by accounting for all other sources of error and assigning the remaining positive error to that caused by blowoff.

A sample calculation is made using the data obtained from shot No. 2: The output voltage of the bridge circuit is shown in figure 16. The distortion of the lower half of the wave train is due to the dc offset. The dc offset is used so that maximum accuracy can be obtained from the positive portion of the waveform. The magnitude of the first peak is 7.8×10^{-3} volts.

The deflection, x , is calculated

$$x = \frac{e_o}{k_1} = \frac{7.8 \times 10^{-3}}{9.17 \times 10^{-2}} = 8.50 \text{ m}$$

m_1 is calculated using formula

$$m_1 = \frac{m_2^{1/2}}{v_1} [kx^2 + 2(K_g + K_w - K_b)]^{1/2} \quad (21)$$

For shot number 1;

$$m_1 = 5.80 \times 10^{-6} \text{ kg}$$

$$v_1 = 6.264 \times 10^3 \frac{\text{m}}{\text{sec}}$$

$$m_2 = 31.0 \times 10^{-3} \text{ kg}$$

$$k = 2.12 \times 10^3 \text{ N/m}$$

$$K_g = 1.20 \times 10^{-5} \text{ Joules}$$

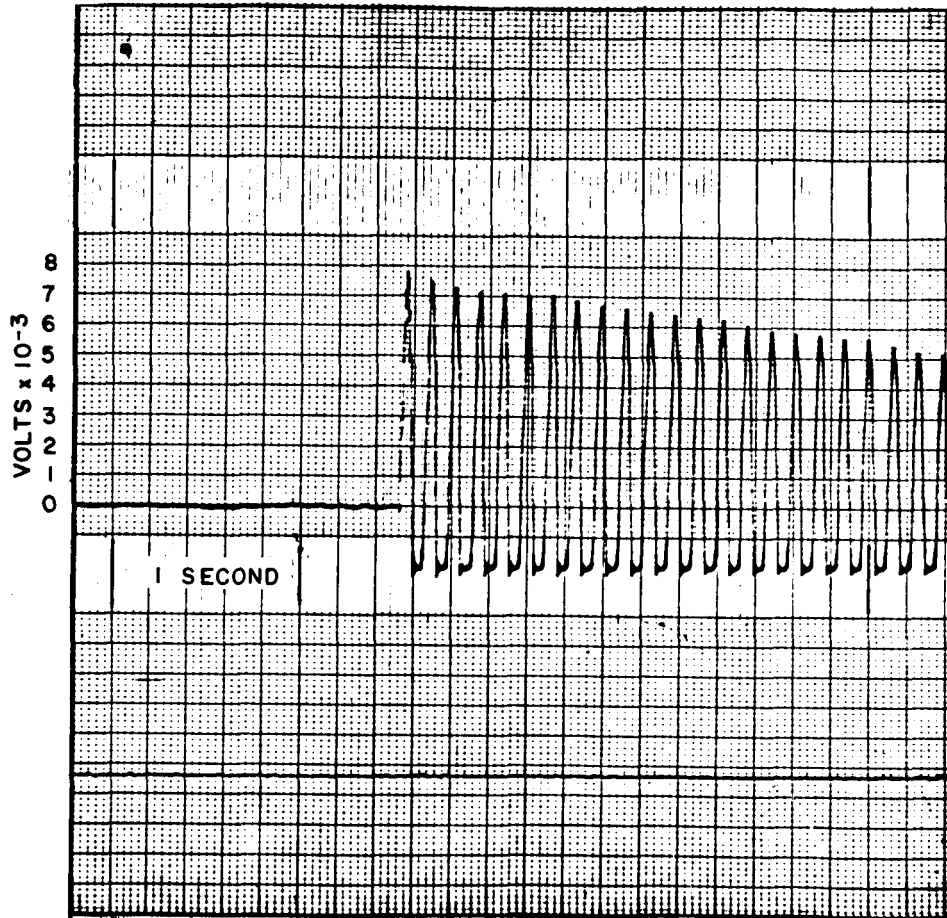
$$K_w = 70 \times 10^{-7} \text{ Joules}$$

$$K_b = \text{unknown}$$

$$\begin{aligned} m_1 &= \frac{31.0}{6.264 \times 10^5} [2.12 \times 10^6 (8.50 \times 10^{-2})^2 + 2(120 + 70)]^{1/2} \\ &= 6.20 \pm \begin{matrix} .28 \\ .29 \end{matrix} \times 10^{-6} \text{ kg} \end{aligned}$$

Table I summarizes the results of the 10 light gas gun shots. Figure 17 is a plot of calculated mass vs. shot number. From this data the mean value for m_1 is calculated to be 6.13×10^{-6} kg which is 5.7% high. It is reasonable to assume after considering all other sources of error, that this positive offset is caused primarily by the blowoff from the projectile impact since a positive thrust would result from the ejected mass.

If to each data point there is applied a correction factor of -0.33×10^{-6} kg, then the deviation of the nominal value about 5.80×10^{-6} kg is within $\pm 5.5\%$.



86-9095

Figure 16 SANBORN RECORDING OF BRIDGE OUTPUT VOLTAGE, SHOT NO. 1

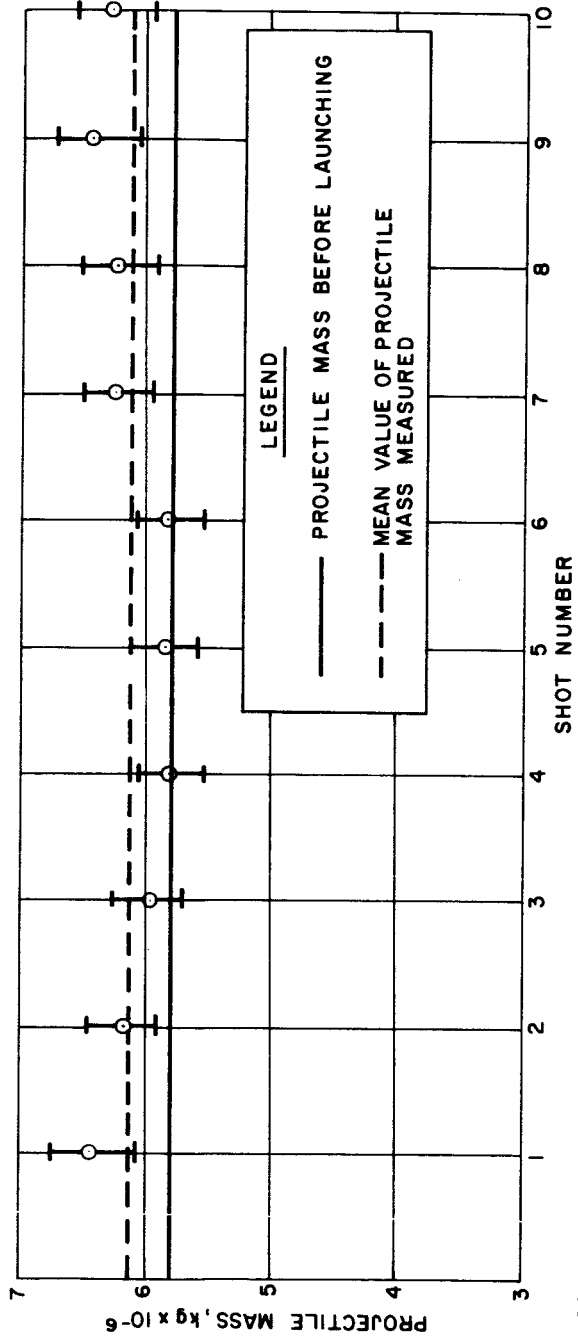


Figure 17 MEASURED MASS VERSUS SHOT NUMBER

7.0 EXPLODING FOIL GUN

The Avco exploding foil gun was used to test the final instrument in an environment similar to that for which it was designed. Initially, some difficulty was encountered from the plasma generated by the exploding foil. Baffles placed downstream near the target tank effectively eliminated the effect of the plasma on the thrust-table reading.

During discharge of the capacitor, a mechanical shock was generated in the structure which produced a large noise pulse in the bridge output. A flexible copper bellows placed between the target tank and the range pipe eliminated this source of noise.

The velocity of the projectile was determined photographically by use of a double pulse Kerr cell shadowgraph system. Two exposures on the same negative of the in-flight projectile are made at fixed known times. The distance the projectile moves is determined directly by measuring the spacing of the two images. The optical gain of the system is a known constant.

Figure 18 is a photograph of the Avco exploding foil gun facility with the mass measuring system installed. Instrumentation for the readout of the strain gage bridge is located in the screen room to the left of the capacitor.

A number of shots was made in the exploding foil gun facility with capacitor voltages of 40 kv, 70 kv and 100 kv. Projectile breakup at voltages of 70 and 100 kv was a problem not overcome during the development of the thrust table. The results of shot No. 89 are discussed. Charging voltage was 40 kv and projectile velocity was 4.2×10^3 m/s. The double pulse Kerr cell photograph from which the velocity is obtained is shown in figure 19. The bright horizontal lines are caused by the lens effect of the glass range pipe on the collimated light of the shadowgraph. Figure 20 is a photograph of the impact plate for this shot. Two large holes and a number of smaller holes suggest that the projectile broke up after the velocity photographs were obtained.

Using equation (16), the mass of the projectile is calculated. The table movement, x , is calculated from equation (20) using the output voltage, $e_o = 6.8$ mv obtained from figure 21.

$$x = \frac{6.8 \times 10^{-3}}{9.17 \times 10^{-2}} = 7.42 \times 10^{-4} \text{ m}$$

The elastic potential energy is calculated

$$\begin{aligned} K_e &= k x^2 = 2.12 \times 10^6 (7.42 \times 10^{-2})^2 \\ &= 1.17 \times 10^{-1} \text{ N} \end{aligned}$$

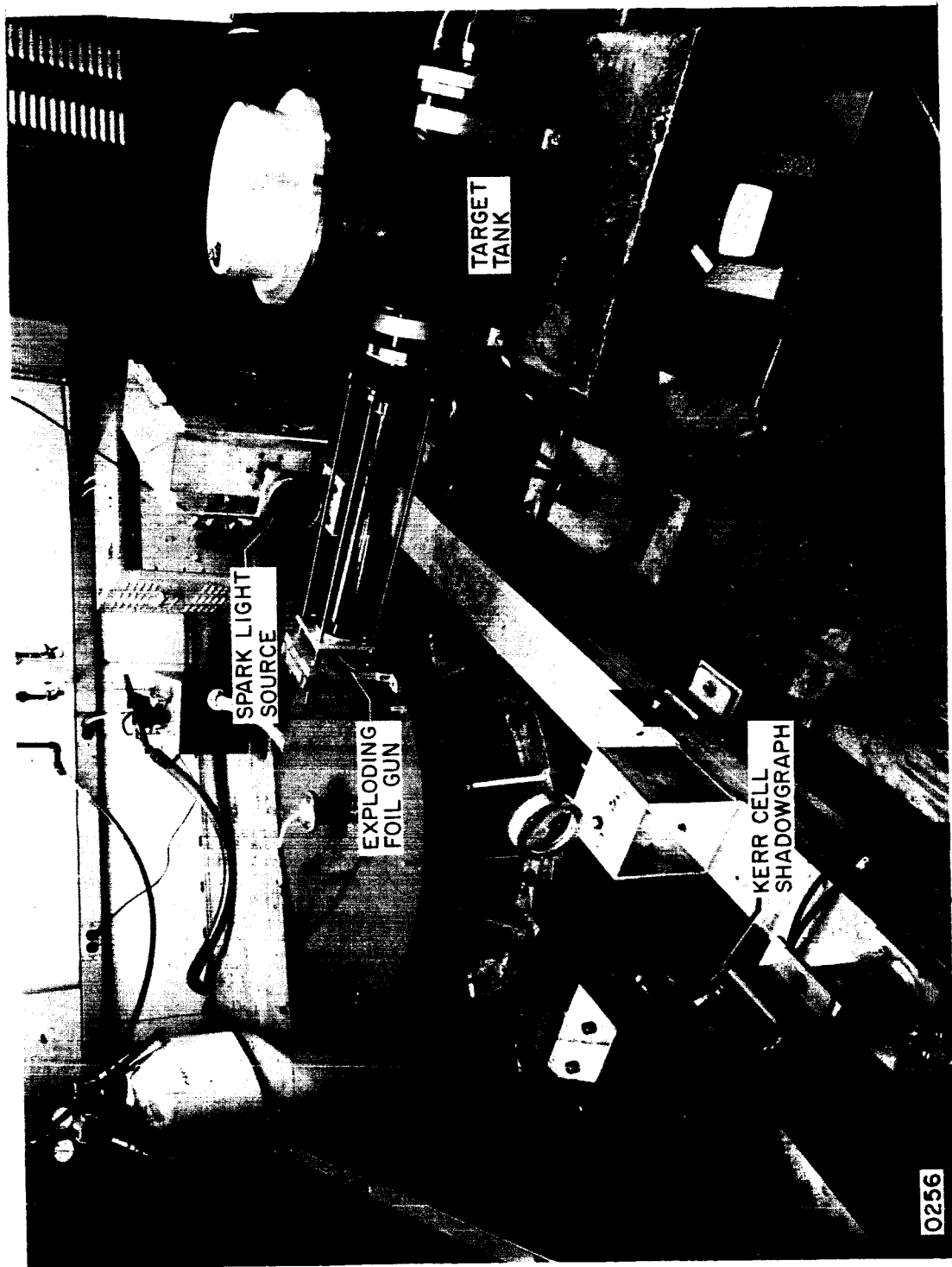


Figure 18 EXPLODING FOIL GUN FACILITY

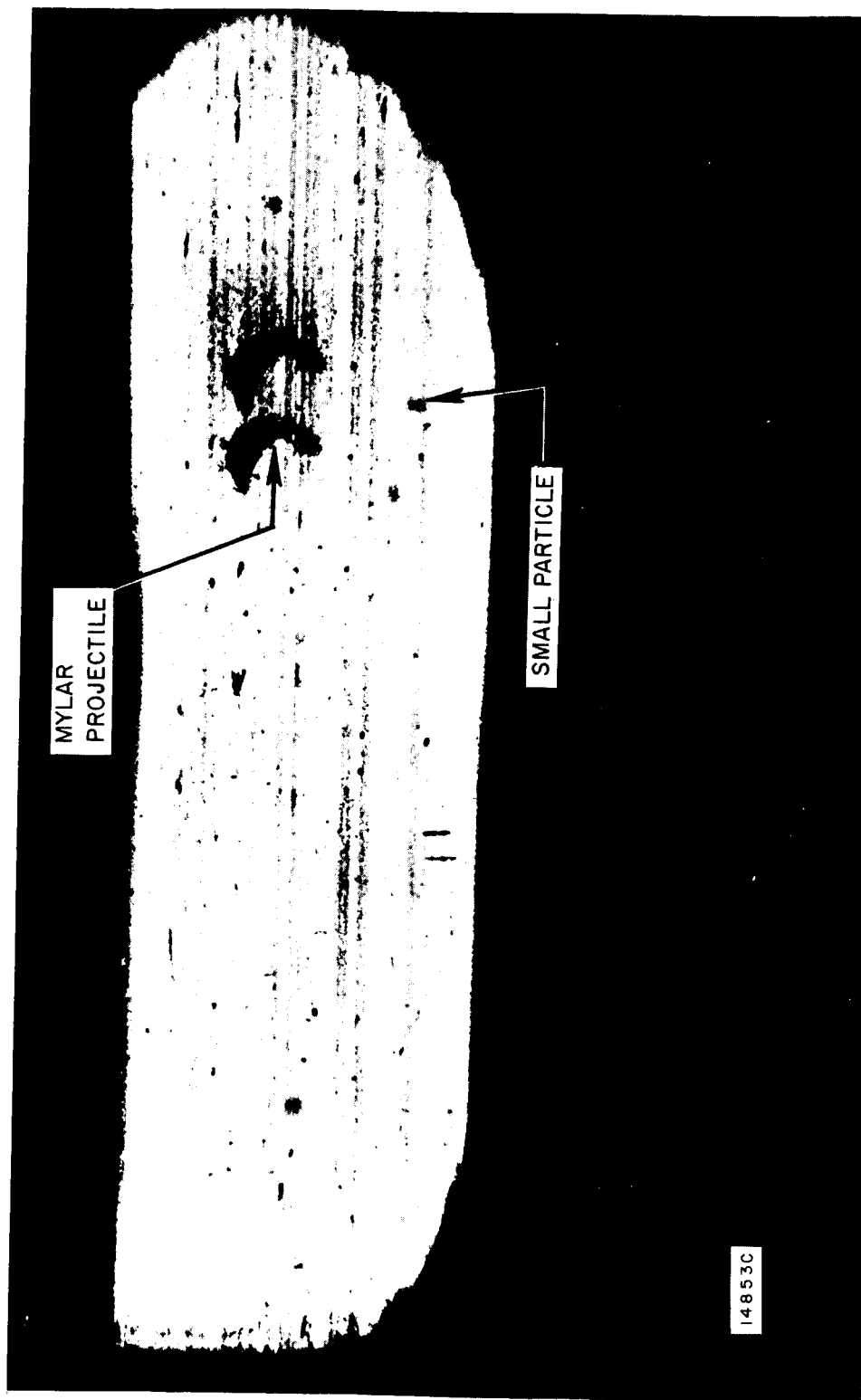


Figure 19 DOUBLE PULSE KERR CELL SHADOWGRAPH



14853 B

Figure 20 IMPACT PLATE

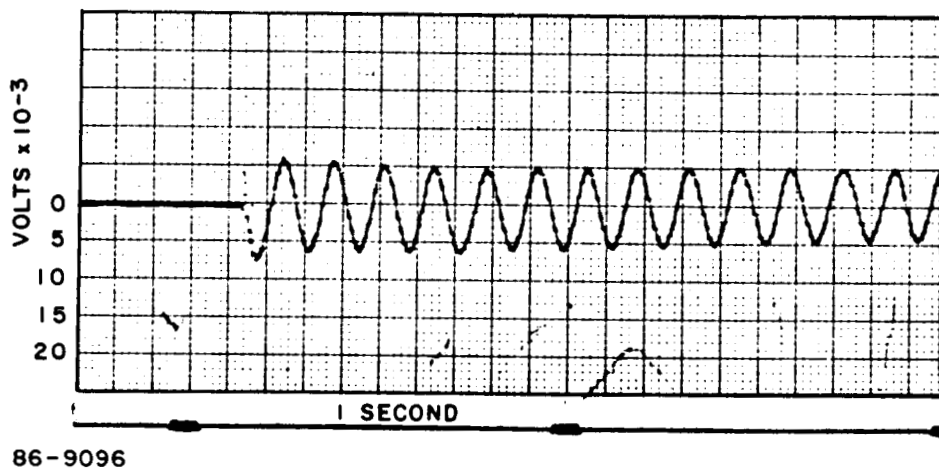


Figure 21 SANBORN RECORDING OF EXPLODING FOIL GUN SHOT

The gravitational potential energy is estimated using figure 10 as 0.8%

$$K_g = 93 \times 10^{-5} \text{ N}$$

A pessimistic estimate of the kinetic energy due to blowoff would be 5% of the elastic potential energy, this value being that obtained from the light gas gun data. This is considered overly pessimistic since the blowoff is a direct function of the impact velocity and the velocity of the exploding foil gun shot was 20% less than the light gas gun shots. A more realistic estimate would be 4% K_e for this exploding foil gun shot.

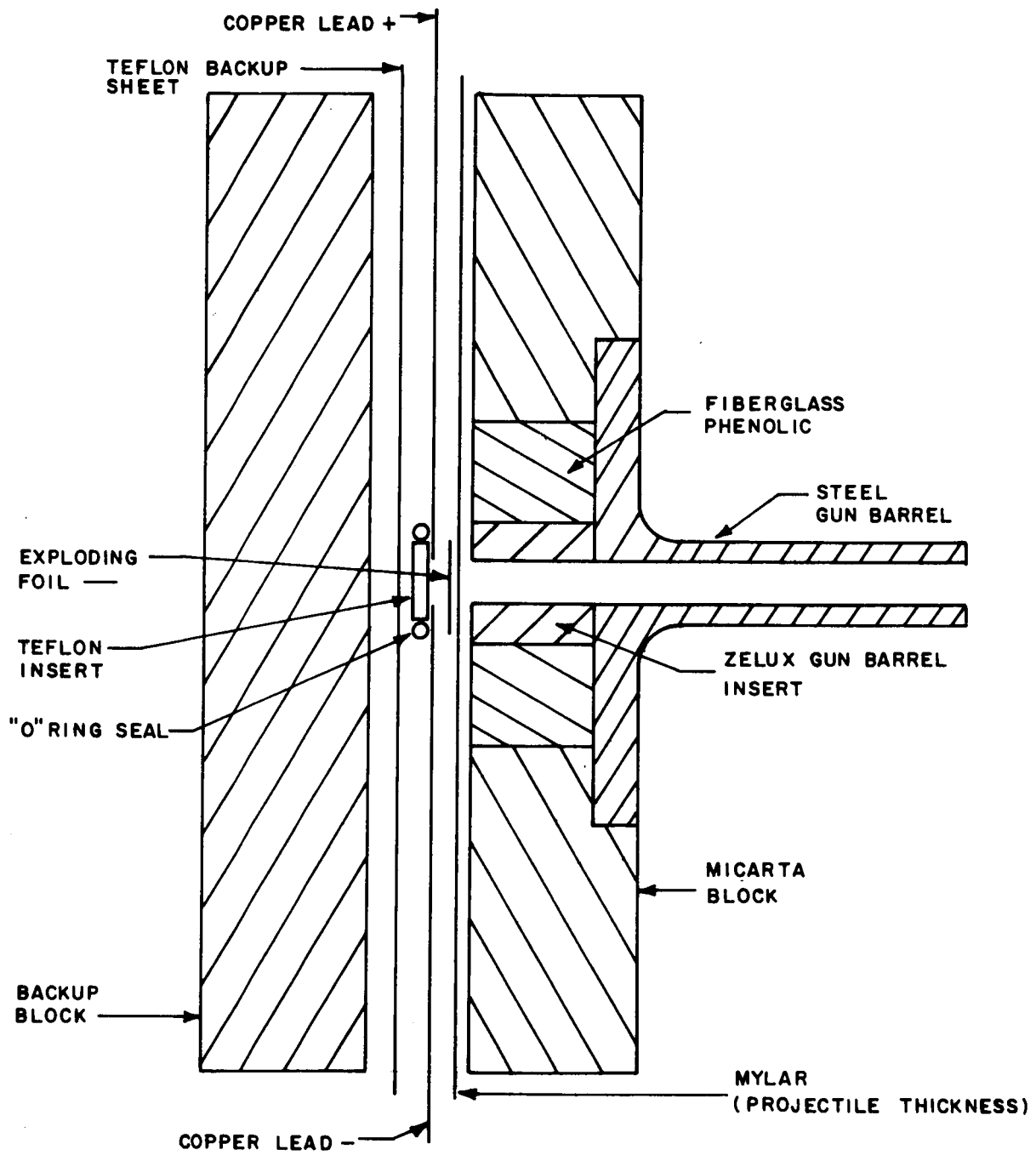
$$\begin{aligned} K_b &= 4\% K_e = 0.04 (1.17 \times 10^4) \\ &= 4.68 \times 10^{-3} \text{ N} \end{aligned}$$

Using equation (16), the mass of the projectile, m_1 , is calculated:

$$\begin{aligned} m_1 &= \frac{31}{4.2 \times 10^5} [2.12 \times 10^6 (5.5 \times 10^{-7}) + 2(93 - 468)]^{1/2} \\ &= 7.7 \text{ mg} \end{aligned}$$

The projectile was a 0.635-cm diameter, 10-mil (2.54×10^{-5} m) thick mylar with an estimated mass of 10 mg. The low reading of the thrust table is probably due to the fact that some of the projectile particles after breakup were caught by the baffles before they reached the impact plate.

During testing in the exploding foil gun facility, it became apparent that due to the relatively long time constant of the thrust table (natural frequency 25 Hz), range vacuum had to be maintained after the shot. Certain gun designs that disintegrate with the launching of the projectile produces a large pressure pulse which has a force many times that of the projectile impact. To circumvent this problem, the Avco exploding foil gun is supplied with the system. This design, shown in cross section in figure 22, will maintain range vacuum with discharge voltages of up to 100 kv.



86-8470

Figure 22 EXPLODING FOIL GUN

8.0 OPERATING INSTRUCTIONS

1. Connect control panel to the thrust table and allow 1/2 hour warmup.
2. Measure "voltage test" after 1/2 hour warmup. This voltage should read 35.0 volts. If it does not, then the bridge sensitivity, k_1 , should be modified a proportionate amount. For example, a reading of 34 volts will produce a new bridge sensitivity $k_1' = \frac{34}{35} k_1$
3. The thrust table should be leveled so that the dc static bridge output voltage is zero when the bridge balance potentiometer is set at 455.5
4. Install impact plates in the target chamber with a small vent hole in each plate. Tighten the target cap screw securely. For consistent results, use the same number of plates and retainers for every shot. Should the projectile catcher mass m_2 be changed to m_2' the factor $(m_2)^{1/2}$ in equation (16) must be changed accordingly to $(m_2')^{1/2}$.
5. Connect a recorder to the "Bridge output" terminals and record the output voltage, e_o , when the target is impacted. From the magnitude of the first peak, read e_o and calculate, x , the distance the table moves from equation (20).

$$x = \frac{e_o}{k_1} = \frac{e_o}{9.17 \times 10^{-2}}$$

6. Calculate the elastic potential energy from

$$K_e = k x^2 = 2.12 \times 10^6 x^2$$

7. Determine the gravitational potential energy, K_g , as a percentage of K_e from figure 10 using the value of x determined in step 5.
8. An estimate is made for K_b and is subtracted from K_g .
9. v_1 is determined from the range instrumentation and m_1 is calculated from equation (16).

$$m_1 = \frac{m_2^{1/2}}{v_1} [k x^2 + 2(K_g - K_b)]^{1/2}$$

$$k = 2.12 \times 10^6 \quad m_2^{1/2} = 31.0$$

The value for m_2 is valid only when the target supplied with the instrument is used. If a target of different mass is used, then the value of m_2 should be modified accordingly. The range of momentum transfer can be extended by increasing the mass of the target. It should be noted that the gravitational potential energy correction would also have to be adjusted accordingly.

9.0 CONCLUSIONS

A system to measure the mass of a projectile which has been fired from an exploding foil gun has been fabricated and delivered to NASA Langley. The primary method used is a modified ballistic pendulum in the form of a thrust table with strain gage readout. Accuracy of the system, with certain corrections, is within $\pm 5.5\%$. The system was tested in the .22 caliber light gas gun range and the Avco exploding foil gun facility with good results.

The thrust generated by the blowoff from the high energy impact presented an error which could not be measured directly or completely eliminated in the time allowed in this program. The design of a multiplate, chambered target reduced the blowoff error considerably and it is felt that additional work in this area could reduce the blowoff error further.

The system will not function with a gun design that does not maintain range vacuum after projectile launch. An Avco gun which maintains range vacuum when operated up to 100 kv is supplied with the system.

The calorimetric method for determining the mass by measuring the kinetic energy of a projectile of known velocity was investigated and found to be impractical due to the difficulty in controlling the heat losses.

10.0 RECOMMENDATIONS

Techniques to reduce the effects due to blowoff should be investigated further in order to realize the full potential of the thrust table. A refinement of the multiplate target is suggested with emphasis placed on capturing more of the energy in the vaporized material generated at impact.



research and advanced development division
201 Lowell Street · Wilmington, Mass.

LABORATORY DATA SHEET

TITLE OF TEST

Static Calibration Final Model. Bridge Sensitivity, k₁

TEST WORK ORDER NO. G178		LABORATORY TEST PLAN NO.			DATA SECURITY CLASS None		
Deflection, x, m ± 5 x 10 ⁻⁶	e ₀ , Volts x 10 ⁻³	$\frac{m}{v}$ x 10 ⁻¹		e ₀ , Volts x 10 ⁻³	$\frac{m}{v}$ x 10 ⁻¹		
0.0254	2.35 ± .01	1.08		2.32 ± .01	1.10		
0.0635	5.81 ± .01	1.09		5.76 ± .01	1.10		
0.127	11.61 ± .01	1.09		11.58 ± .01	1.10		
0.254	23.30 ± .01	1.10		23.29 ± .01	1.09		
0.508	46.74 ± .01	1.09		46.76 ± .01	1.09		
0.761	70.47 ± .01	1.08		70.54 ± .01	1.08		
1.02	94.40 ± .01	1.08		94.35 ± .01	1.08		
Bridge Supply Voltage, E = 35 Volts							

REMARKS:
e₀ monitored with Fluke 803D Differential Voltmeter No. 757
E supply voltage to bridge monitored on Weston Model 622 No. 19180
Displacement monitored with Starret Micrometer Head No. 263

TEST ENGINEER	DATE	TEST WITNESS	DATE	TEST WITNESS	DATE
J. Amorel	5/4/66				



research and advanced development division
201 Lowell Street · Wilmington, Mass.

LABORATORY DATA SHEET

TITLE OF TEST

Static Calibration Final Model. Spring Constant, k_2

TEST WORK ORDER NO.	LABORATORY TEST PLAN NO.	DATA SECURITY CLASS
G178		None

Force N	e_0 , Volts $\times 10^{-3}$	k_2 N/v $\times 10^2$					
8.90 ± .04	38.03 ± .01	2.34					
8.90 ± .04	38.16 ± .01	2.33					
8.90 ± .04	38.24 ± .01	2.33					
8.90 ± .04	38.32 ± .01	2.32					
8.90 ± .04	38.36 ± .01	2.32					
8.90 ± .04	38.30 ± .01	2.32					
8.90 ± .04	38.27 ± .01	2.33					
8.90 ± .04	38.31 ± .01	3.32					
8.90 ± .04	38.32 ± .01	2.32					
8.90 ± .04	38.31 ± .01	2.32					

REMARKS:

e_0 monitored with Fluke 803D Differential Voltmeter No. 757
 E Supply Voltage to bridge monitored on Weston Model 622 No. 19180
 Force applied with Chatillon Scale model P-P1-2 No. 1739

TEST ENGINEER	DATE	TEST WITNESS	DATE	TEST WITNESS	DATE
<i>J. Morreal</i>	5/6/66				

TABLE I
LIGHT GAS GUN CALIBRATION SHOTS

Shot No.	Projectile Velocity (m/sec x 10 ³)	Output Voltage, e_0 , (volts x 10 ⁻³)	Projectile Mass (mg)	Calculated Mass (kg)	% Error
1	6.329	8.2	5.80	6.44	+11
2	6.264	7.8	5.80	6.20	+7
3	7.124	8.6	5.80	5.98	+3
4	7.170	8.4	5.80	5.81	+0.2
5	7.278	8.6	5.80	5.86	+1
6	7.327	8.6	5.80	5.82	+0.3
7	7.286	9.2	5.80	6.26	+8
8	5.910	7.4	5.80	6.26	+8
9	5.814	7.5	5.80	6.41	+10
10	5.871	7.4	5.80	6.30	+9

TABLE II
GRAVITATIONAL POTENTIAL ENERGY

Horizontal Displacement (mm)	Vertical Displacement (μm)	K_g (Joules)	% Elastic Potential Energy
1.27	2.54 \pm 2.54	2.4 x 10 ⁻⁵	1.4
2.54	20.2 \pm 2.54	1.9 x 10 ⁻⁴	2.8
4.08	71.2 \pm 2.54	6.7 x 10 ⁻⁴	2.4
7.62	173 \pm 2.54	1.5 x 10 ⁻³	2.4
8.16	279 \pm 2.54	2.6 x 10 ⁻³	2.4

TABLE III
THRUST TABLE MASS

Part	Mass (grams)	Total Mass (grams)
End plate	132.6	
End plate	129.5	
Base (box beam)	295.6	
Hardware (nuts and bolts)	36.0	
Clamped portion of flexure	32.4	
Total table top		626.1
Vibrational load flexures	33.5	
Target	295.5	
Total mass, m_2 , without impact plates		955.1
Copper impact plates (6)	6.6	
Total mass, m_2		961.7

APPENDIX

DYNAMIC ANALYSIS OF BASE PLATE - THRUST TABLE SYSTEM

by

R. H. Coco

APPENDIX

SUMMARY

The dynamic analysis described in this release was requested in order to determine the displacement, velocity and acceleration of the base plate due to impact of the projectile with the target. These quantities were necessary to account for the amount of energy loss due to motion of the suspension table. Direct laboratory measurement of these quantities could not be easily accomplished. The results of the analysis are presented in figures A4 through A15 as displacement, velocity and acceleration time histories for both the thrust table and the base plate.

The analytical results for the case $w_p = 5.8$, mg, $v_p = 6,096$ m/s, (figure A4) has been compared with experimental results and show correlation to within 10% of the measured results. The results from future ground test will also be compared with the analytical results predicted here.

Method of Analysis

The desired time histories were found by first reducing the system of figure A2 to an equivalent mathematical dynamic model using the lumped parameter technique. The equations of motion written from this equivalent system were then solved on the IBM 7094 digital computer to yield the desired displacements.

Figure A3 shows the dynamic model for the system of figure A2. The numerical values for the masses, inertias, and spring rates of the model are listed in table AII.

The stiffness values of table AII were provided by test; the inertia values were calculated using known dimensions and material densities.

TABLE AI

CASE STUDIED

v_p Velocity Projectile km/s	w_p Weight Projectile Case I
6,096	a. 5.8 mg

In deriving these equations the following assumptions were made:

- 1) Small displacements theory is valid
- 2) The suspension table support springs, K_s , offer no lateral restraint to motion of the suspension table.

The differential equations (1) were then solved using Avco digital Program 1520G for the desired dynamic responses. The values calculated were then automatically plotted on the SC-4020 plotter and are presented in figures A4 through A15 of this release.

Forcing Function

The forcing function was derived using linear momentum theory. In determining the forcing function the following assumptions were made:

- 1) The force-time history of the forcing function can be represented as a step function of finite duration time, τ . (See figure A1)
- 2) The duration time, τ , is equal to the time required for the projectile to travel a distance equal to one diameter of its length. The diameter of the projectile, 1.59 mm, was measured in the laboratory.
- 3) All of the energy of impact is transferred to the thrust table without loss.
- 4) The weight of the particle is very much smaller than the weight of the thrust table.

With these assumptions considered, the equation of motion for the particle of mass m_p in the x-direction is:

$$F_x = m_p dv/dt \quad (2)$$

Since m_p is constant, equation (2) can be written

$$F = d/dt (m_p v) \quad (3)$$

or

$$F dt = d (m_p v) \quad (4)$$

On integrating (4) for the limits $0 \leq t \leq \tau$ and $0 \leq v \leq v_p$, we have

$$F \tau = m_p v_p \quad (5)$$

then

$$F = m_p v_p / \tau \quad (6)$$

where $v_p \sim$ velocity of the particle \sim m/s

$m_p \sim$ mass of the particle \sim kg

$\tau \sim$ duration of pulse \sim sec

The duration of the pulse, τ , is simply

$$\tau = 1/16/v_p \quad (7)$$

Substituting (7) into (6) yields:

$$F_x = 16 m_p v_p^2 \quad (8)$$

For the case listed in table AI the force, F , was calculated from equation (8) and is given in table AIII.

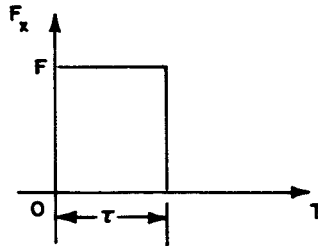


Figure A1 ASSUMED FORCE-TIME HISTORY

TABLE AII
PHYSICAL PARAMETERS OF THE DYNAMIC MODEL

Coordinate	Mass or Inertia	Stiffness
x_1	1.64 kg	$K_b = 5.24 \times 10^2$ (N/m per strut)
θ_1	2.0 n-m-s ²	$K_t = 1.59 \times 10^4$ (N/m per strut)
x_2	47.3 kg	
θ_2	6.45 n-m-s ²	$K_s = 0.335$ (N/m per spring)

The equations of motion written directly from figure A2 are:

$$m_1 \ddot{x}_1 + 4K_b(x_1 - x_2) = F(t)$$

$$I_1 \ddot{\theta}_1 + 4K_t d^2(\theta_1 - \theta_2) = e \{ F(t) \}$$

$$m_2 \ddot{x}_2 + 4K_b(x_2 - x_1) = 0$$

$$I_2 \ddot{\theta}_2 + 4K_t d^2(\theta_2 - \theta_1) + 4K_s l^2(\theta_2) = 0 \tag{1}$$

(\dot{x} terms not shown)

where: x = translation coordinate

θ = rotation coordinate

m_1 = mass of thrust table kg

I_1 = inertia of thrust table N-m-s²

m_2 = mass of suspension table (kg)

I_2 = inertia of suspension table (N-m-s²)

K_b = bending stiffness of struts (N/m)

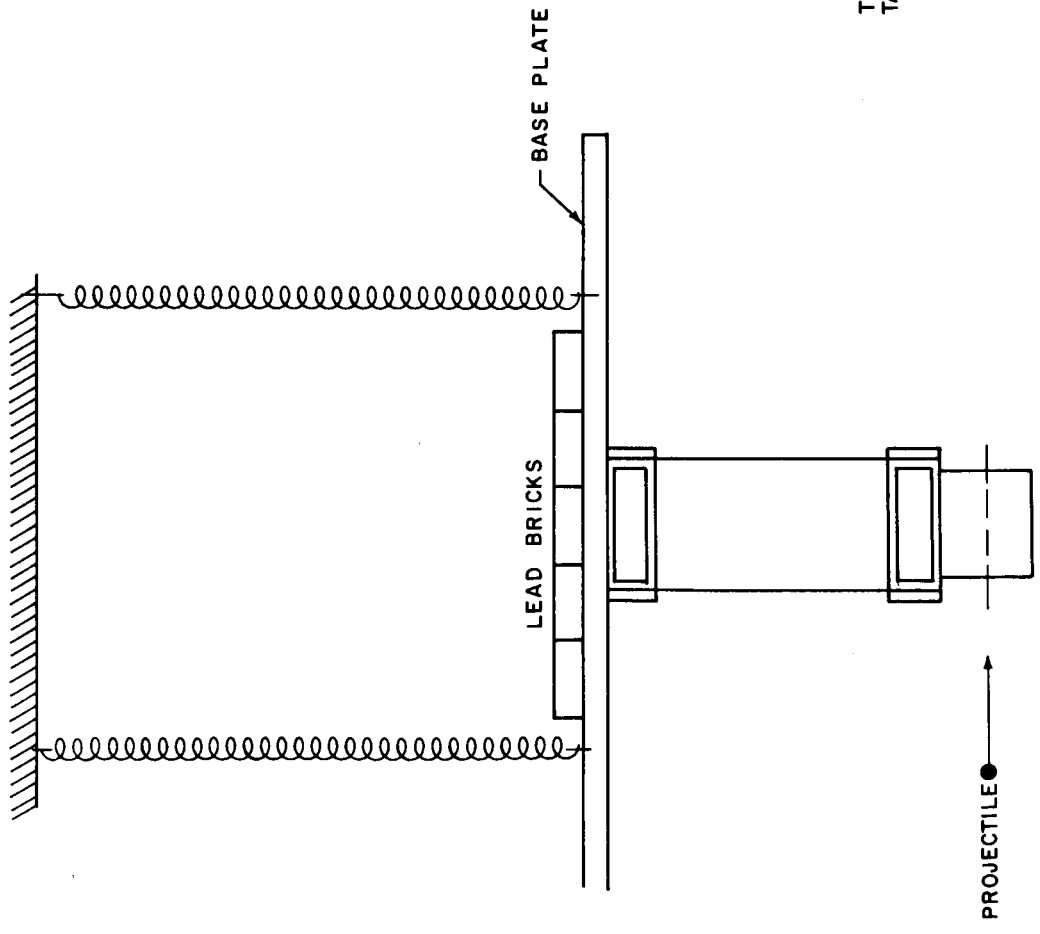
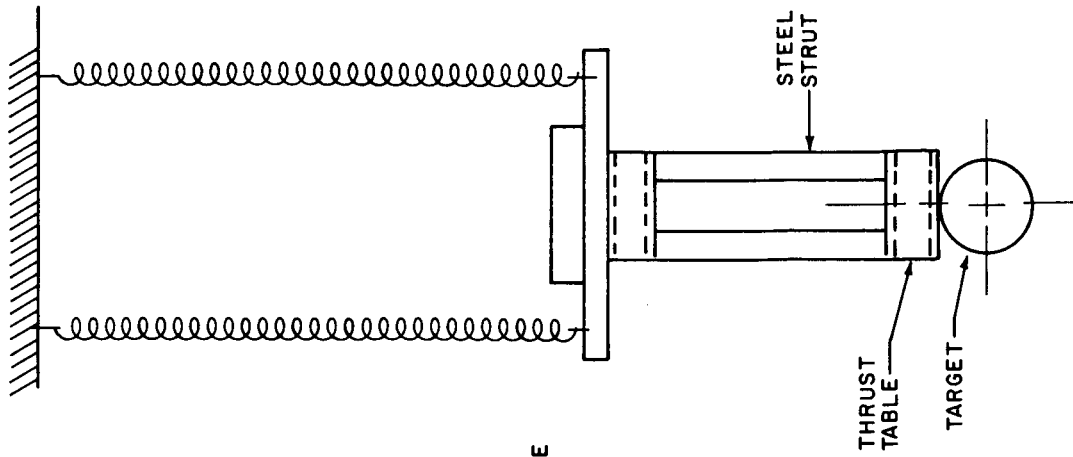
- K_t = tension stiffness of struts (N/m)
 K_s = stiffness of suspension table support (N/m)
 e = eccentricity of forcing function from c. g. of m_1 (m)

TABLE AIII
 FORCE CALCULATIONS FOR CASE I

Velocity, v_p , ft/sec	Case I F, N, (5.8 mg)
6, 096 m/s	$4.4 \times 3.053 \times 10^4$

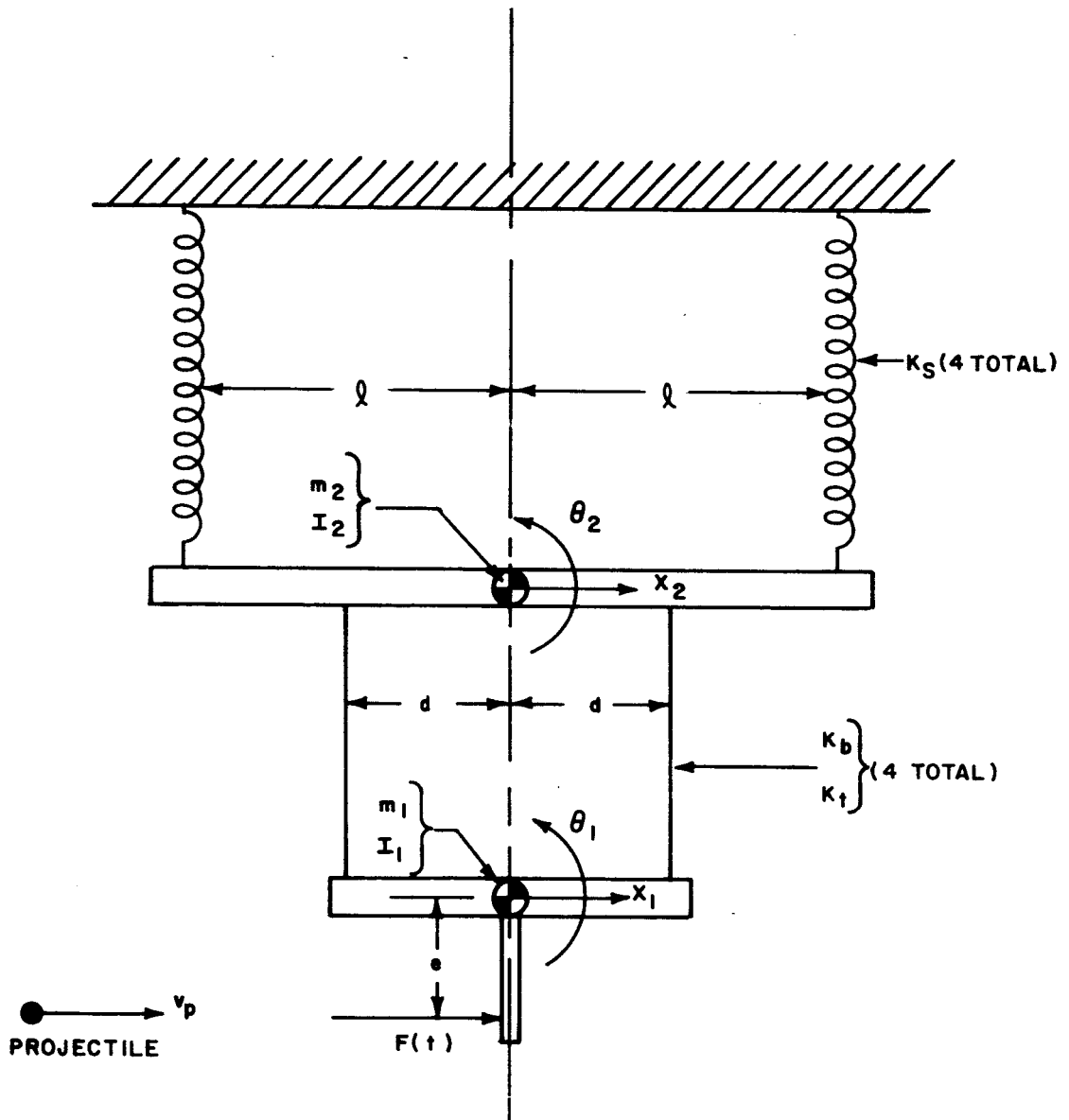
Results

The results of the analysis, presented as plots of displacement $x_1, \theta_1, x_2, \theta_2$, velocities: $\dot{x}_1, \dot{\theta}_1, \dot{x}_2, \dot{\theta}_2$, and accelerations: $\ddot{x}_1, \ddot{\theta}_1, \ddot{x}_2, \ddot{\theta}_2$, versus time for the cases considered are presented in figures A4 through A15.



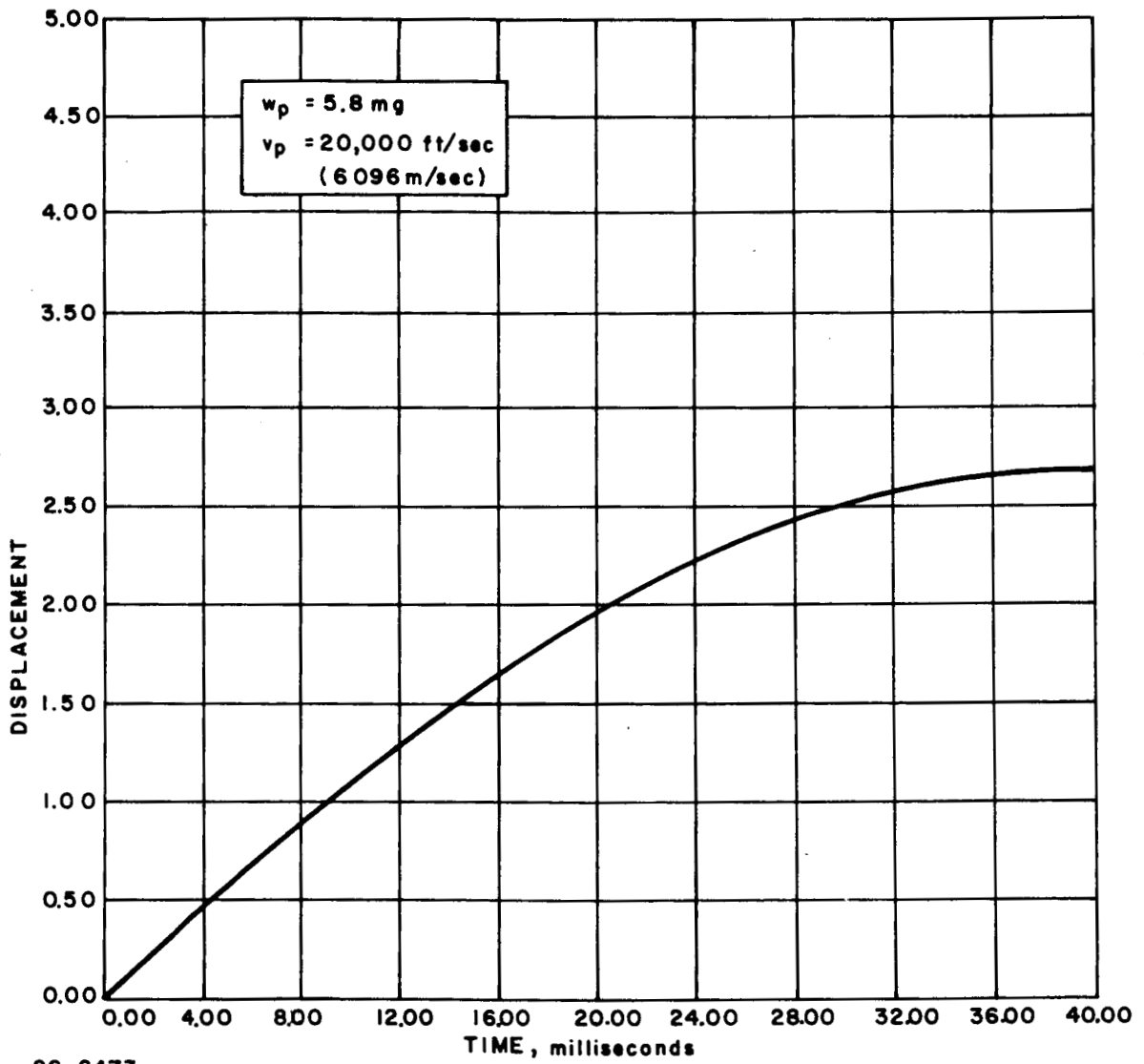
86-8471

Figure A2 SUSPENSION SYSTEM



86-8472

Figure A3 DYNAMIC MODEL OF SYSTEM



86-8473

Figure A4 TRANSIENT RESPONSE CASE 2.1 MEMO 1303.0 COORDINATE $\sim X_1$

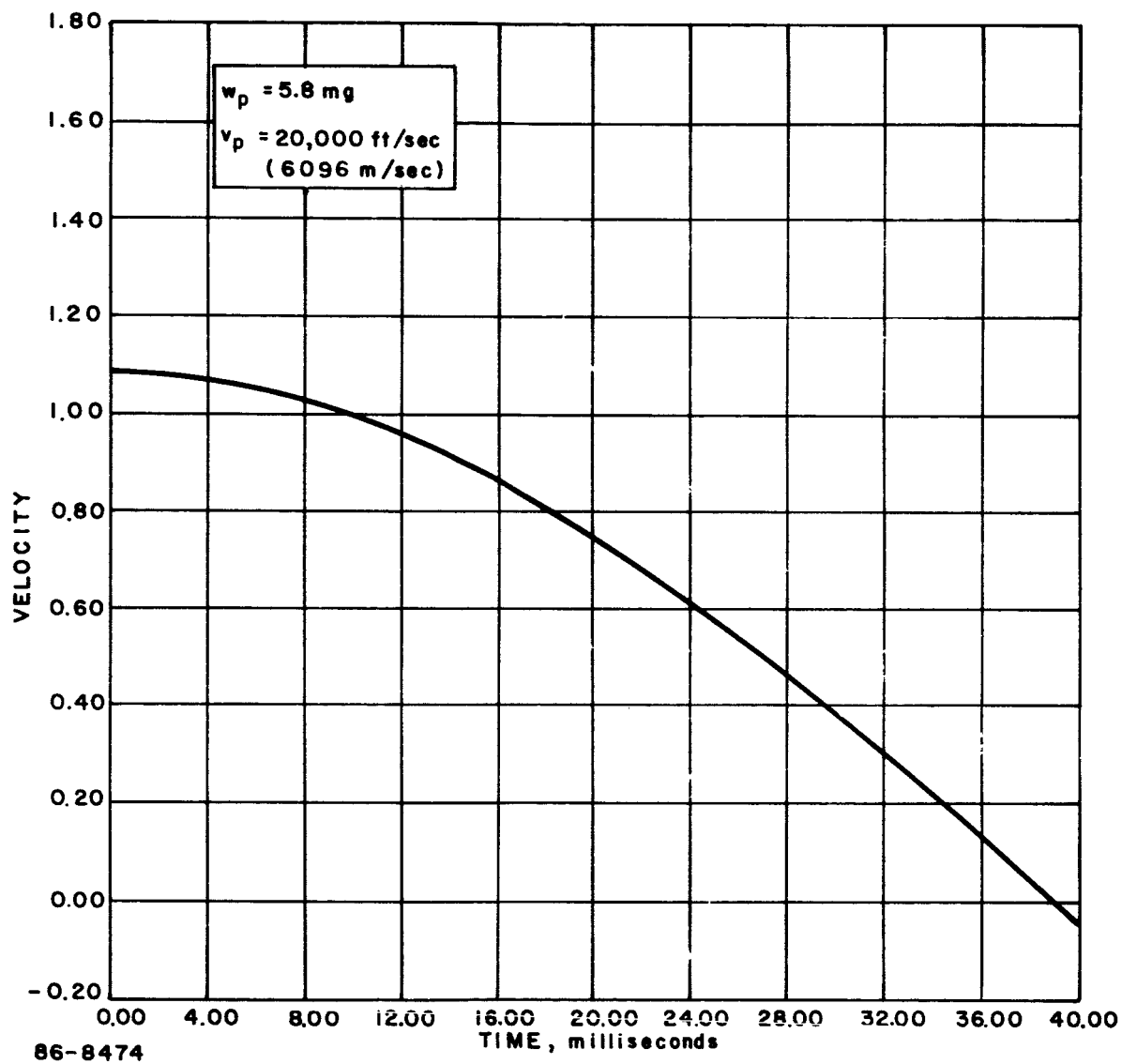


Figure A5 TRANSIENT RESPONSE CASE 2.1 MEMO 1303.0 COORDINATE \dot{x}_1

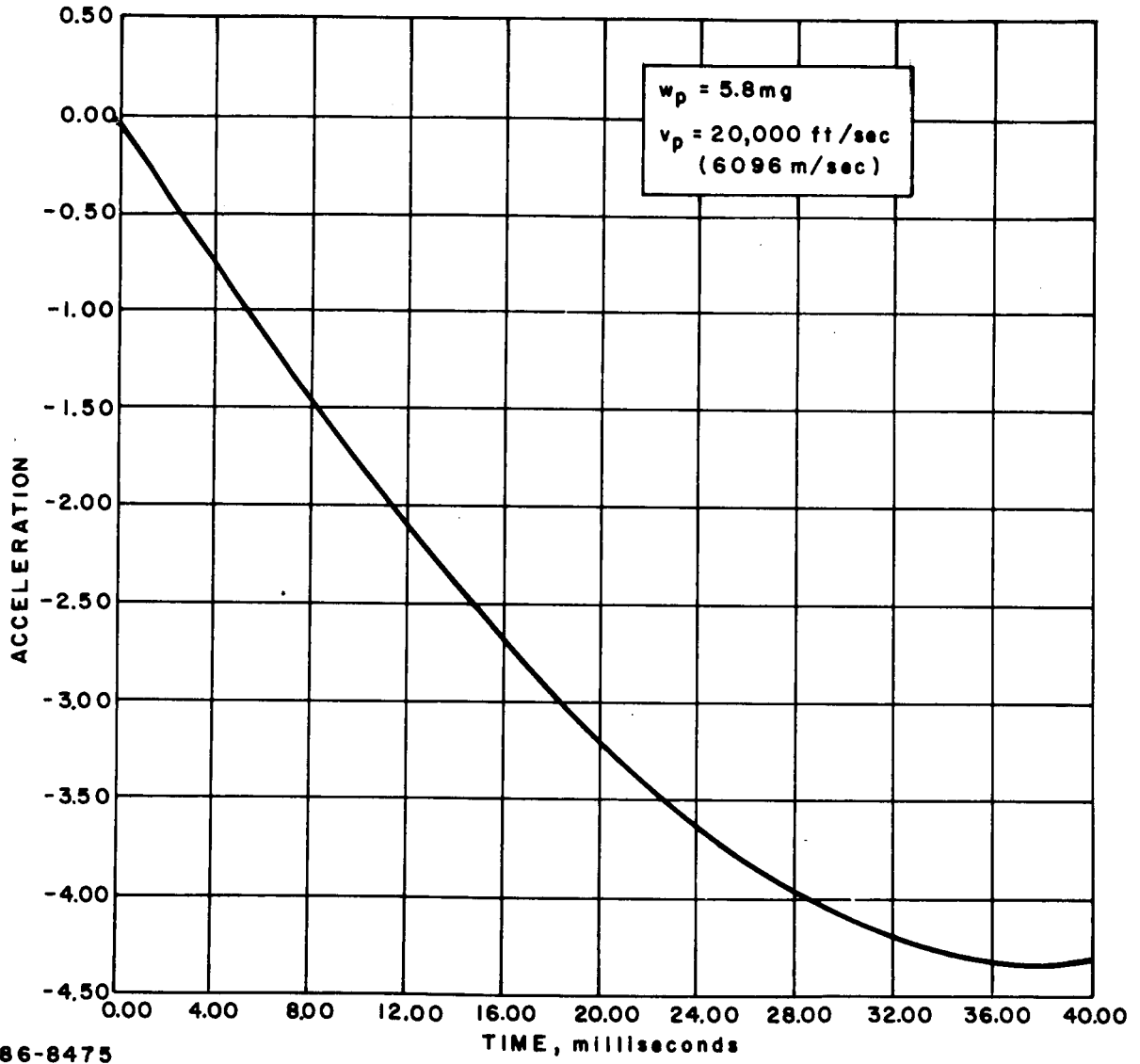


Figure A6 TRANSIENT RESPONSE CASE 2.1 MEMO 1303.0 COORDINATE $\ddot{\chi}_1$

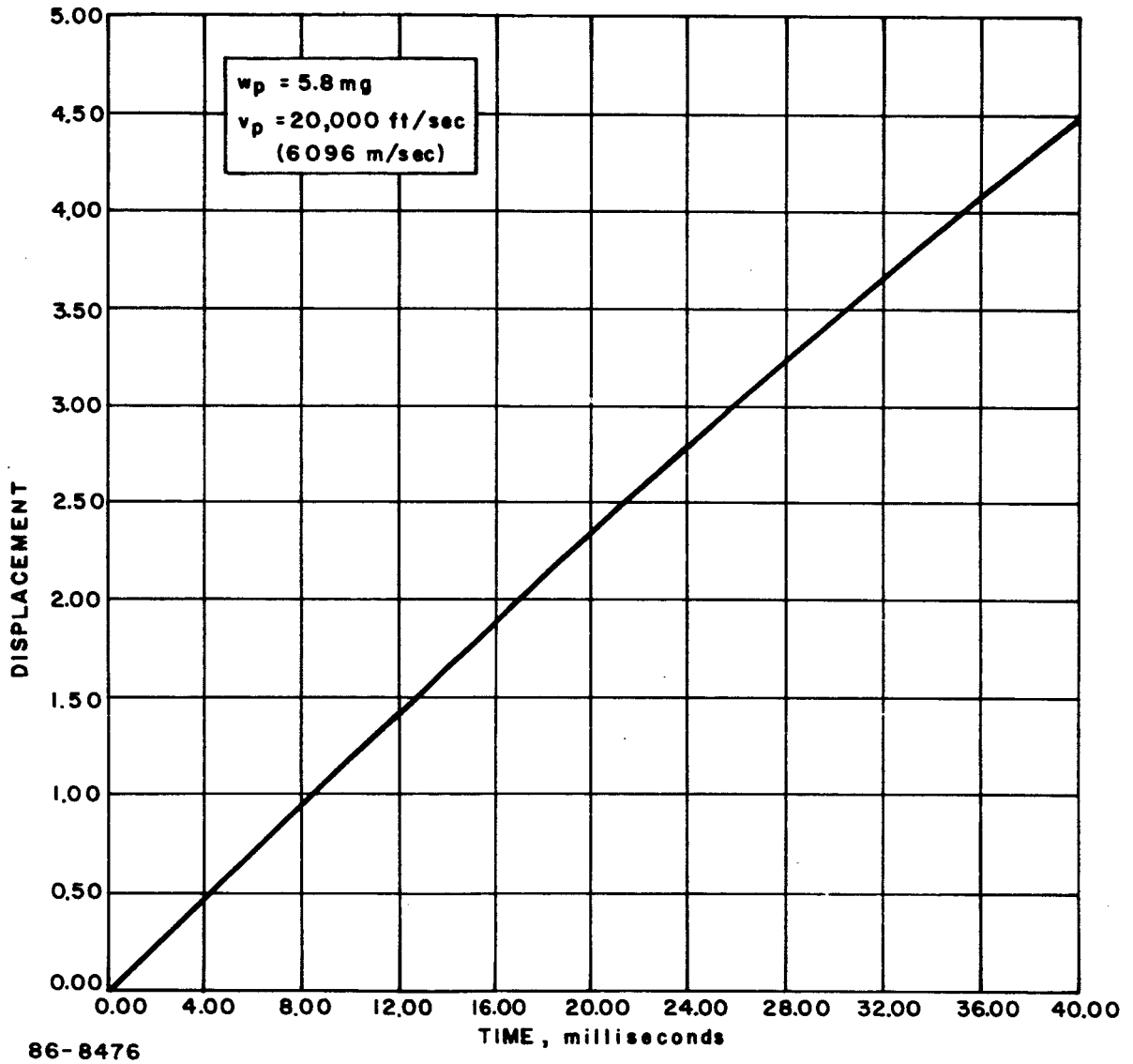


Figure A7 TRANSIENT RESPONSE CASE 2.1 MEMO 1303.0 COORDINATE $\sim \theta_1$

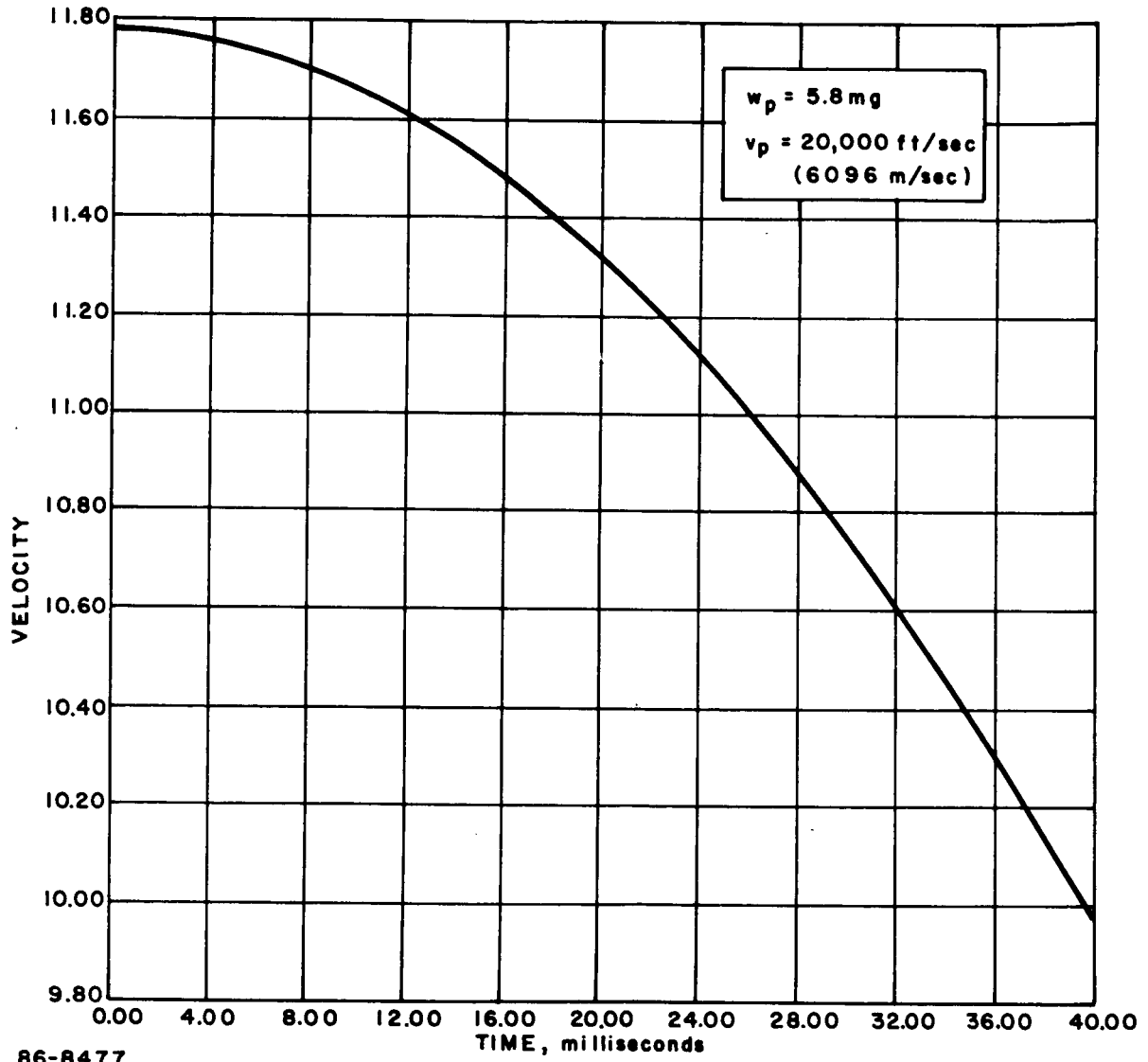


Figure A8 TRANSIENT RESPONSE CASE 2.1 MEMO 1303.0 COORDINATE $\sim \dot{\theta}_1$

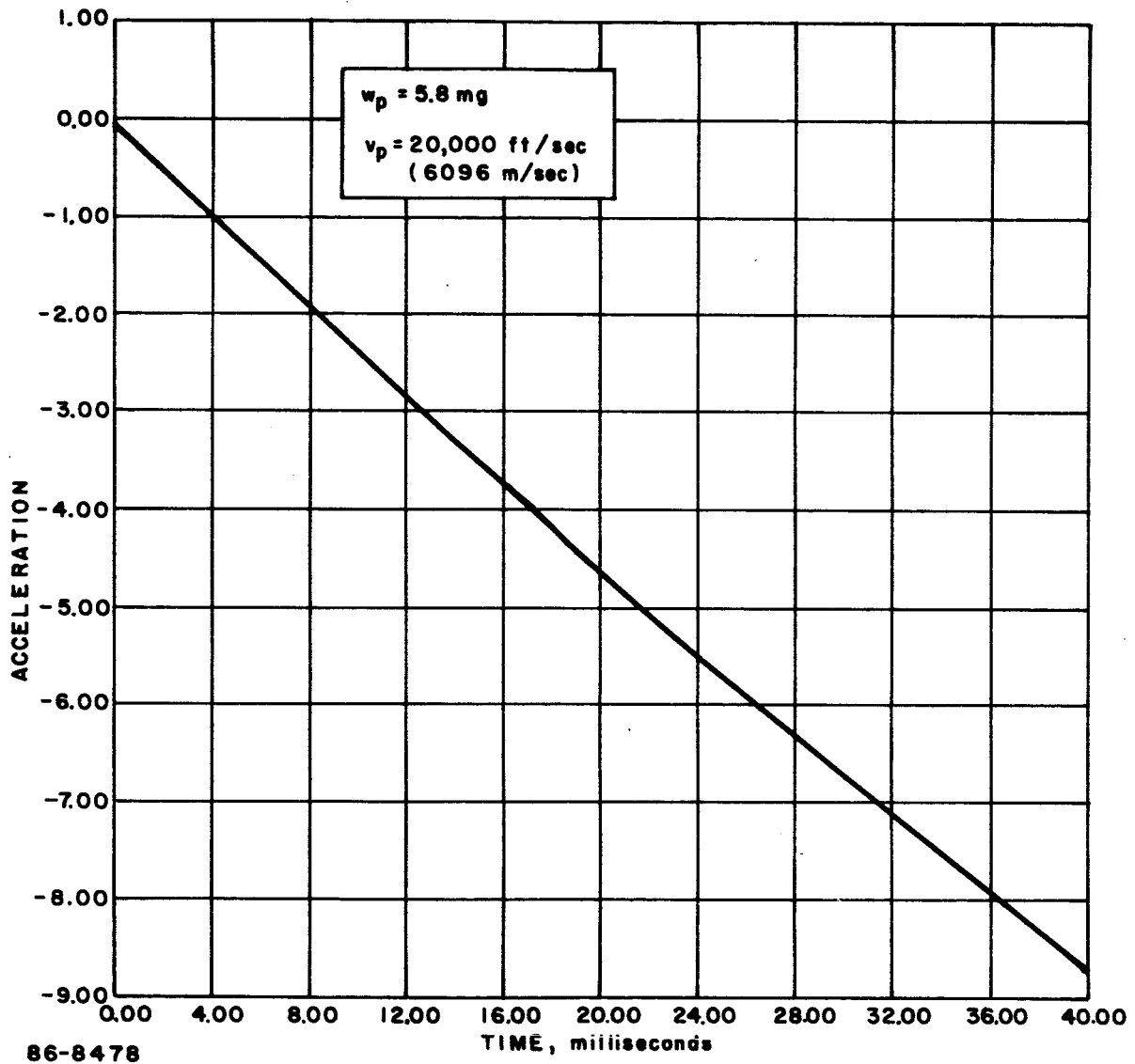
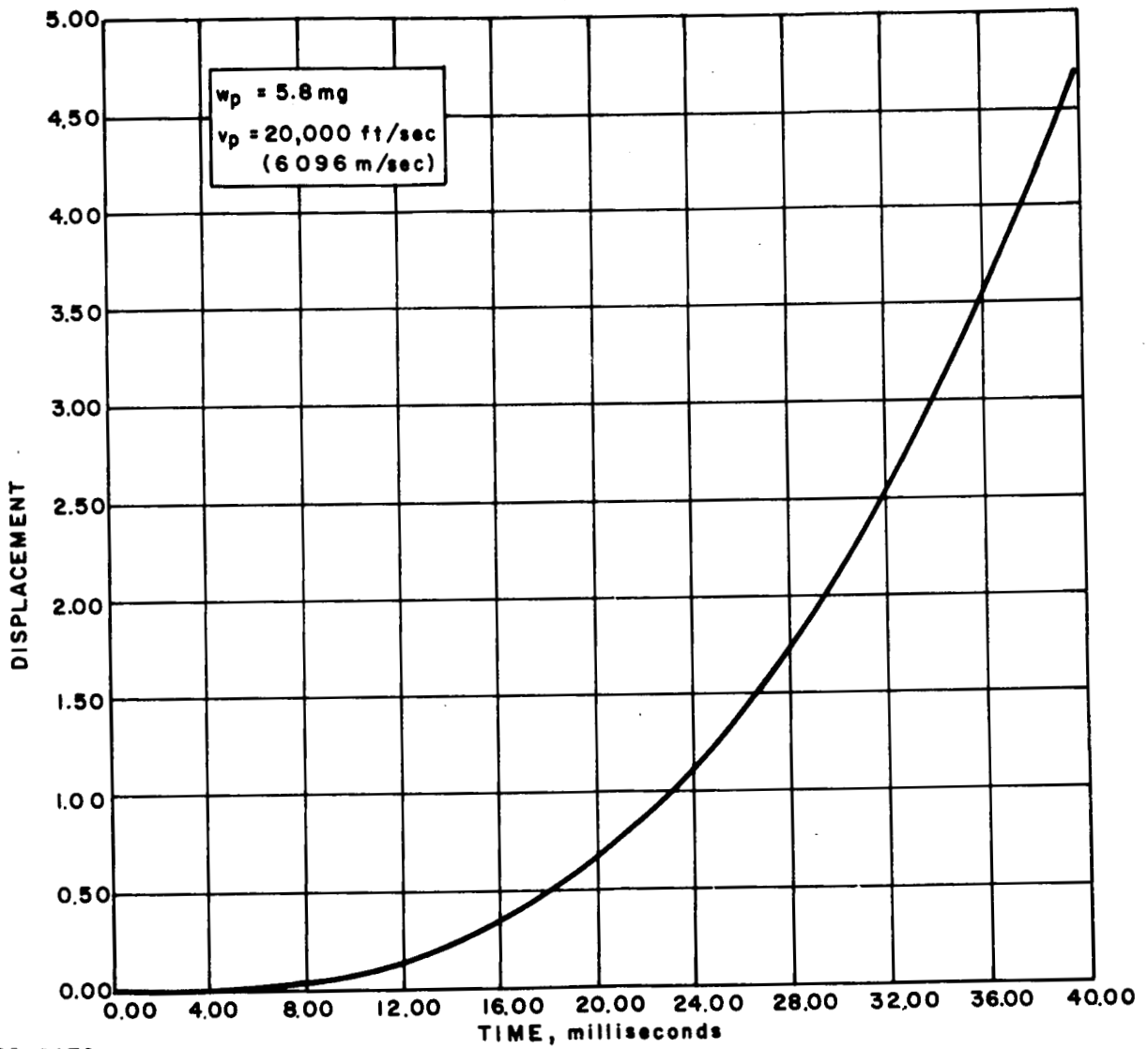


Figure A9 TRANSIENT RESPONSE CASE 2.1 MEMO 1303.0 COORDINATE $\sim \ddot{\theta}_2$



86-8479

Figure A10 TRANSIENT RESPONSE CASE 2.1 MEMO 1303.0 COORDINATE $\sim X_2$

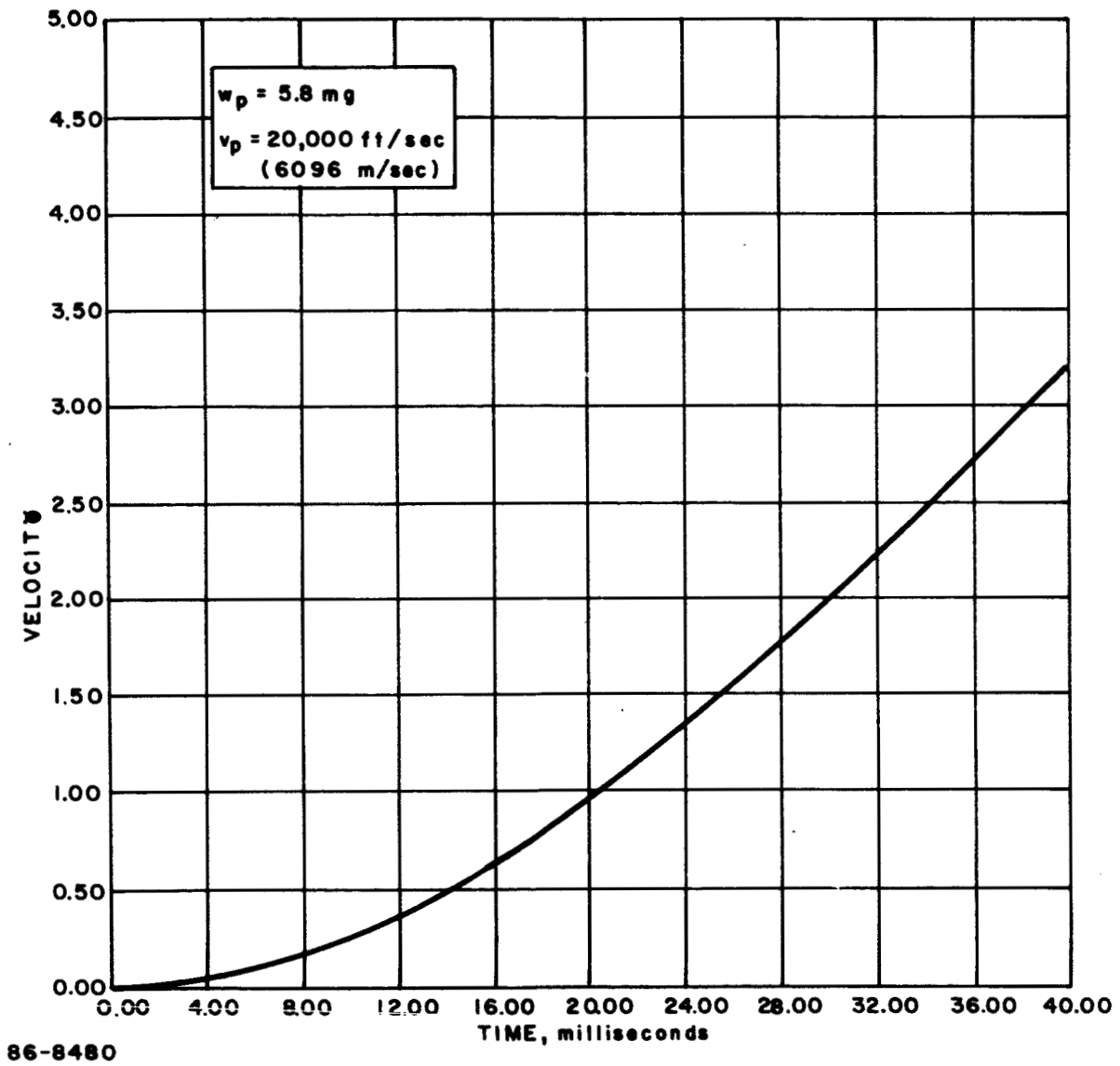


Figure A11 TRANSIENT RESPONSE CASE 2.1 EMO 1303.0 COORDINATE $\sim \dot{x}_2$

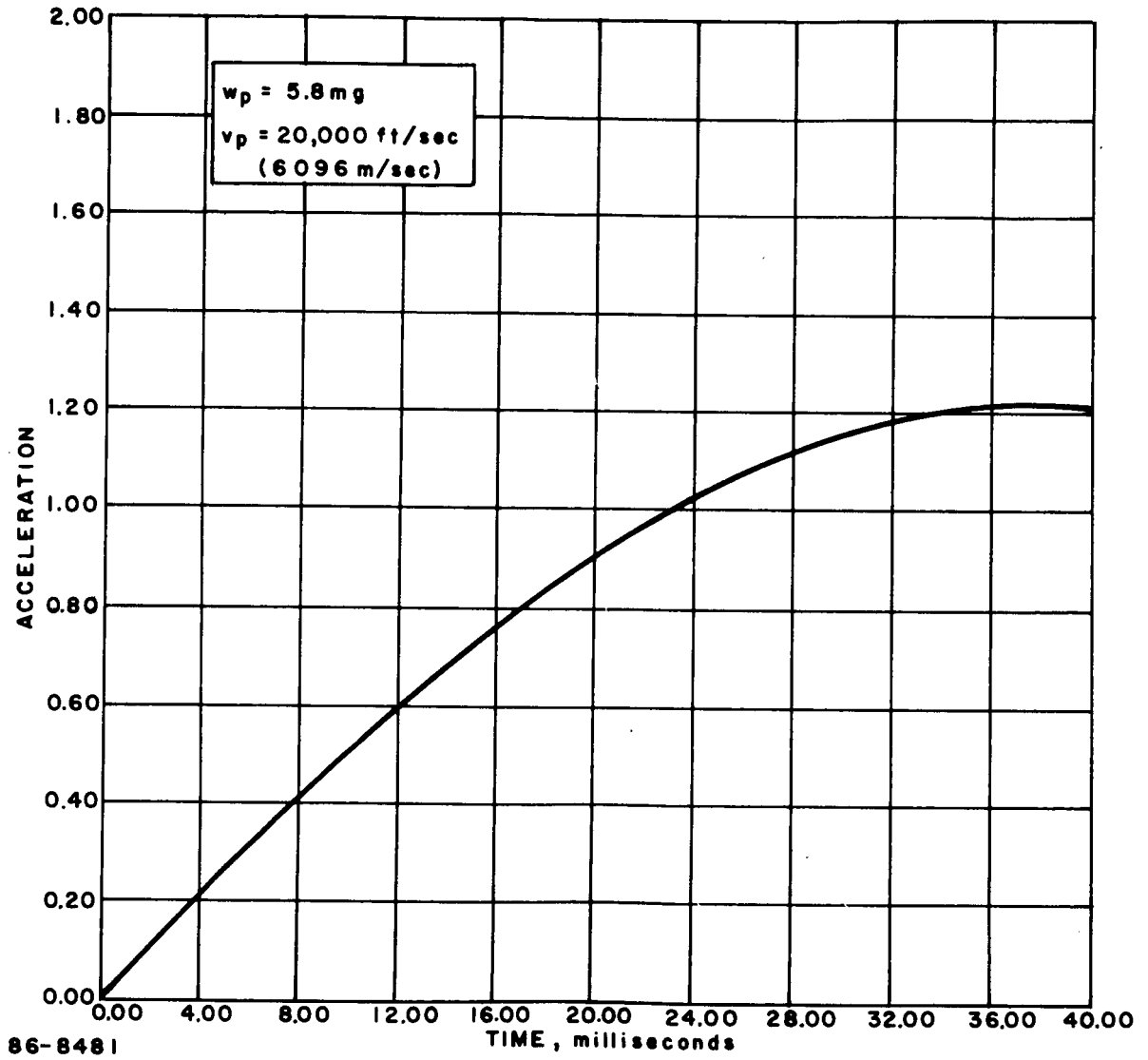


Figure A12 TRANSIENT RESPONSE CASE 2.1 MEMO 1303.0 COORDINATE \ddot{x}_2

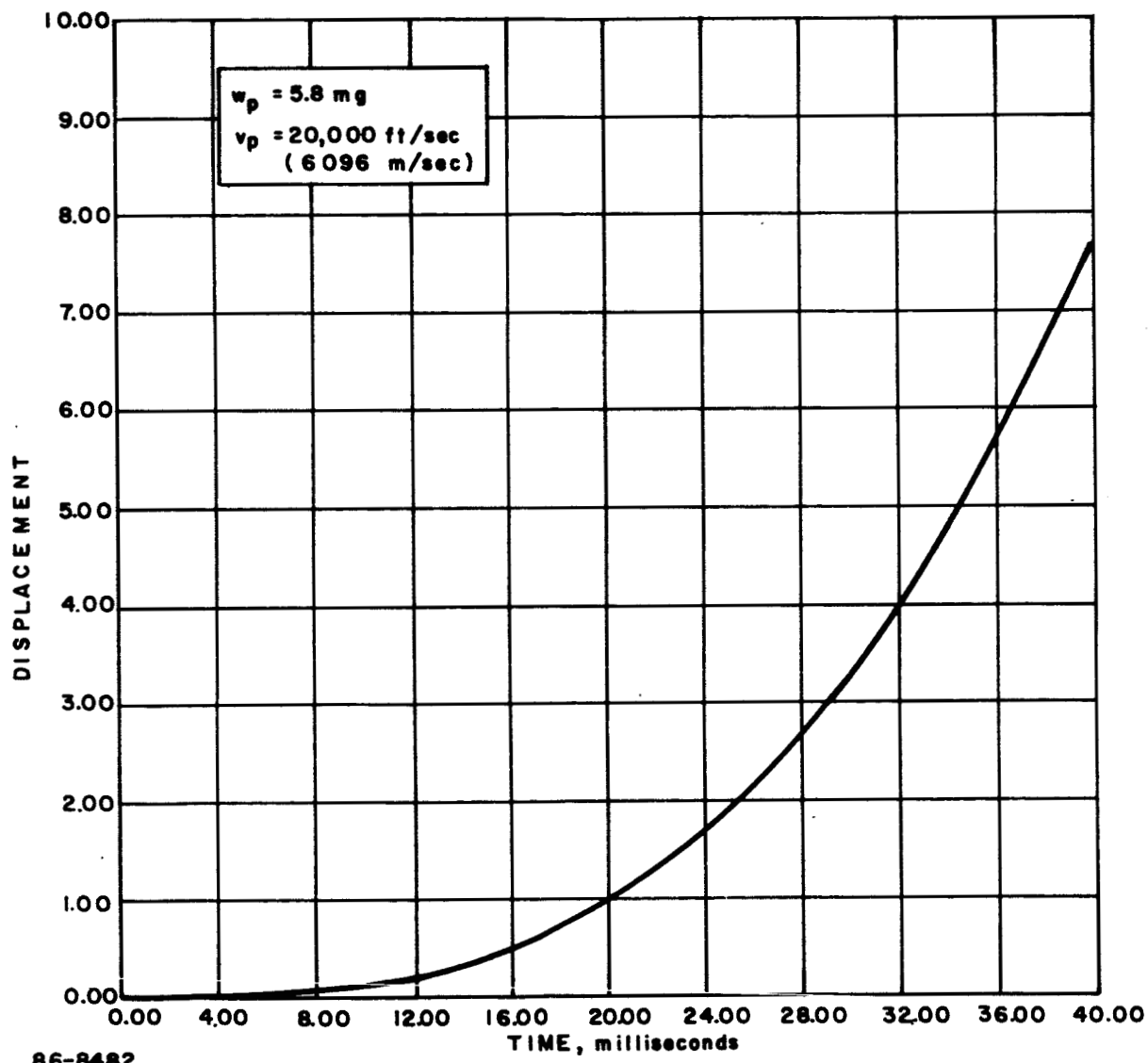


Figure A13 TRANSIENT RESPONSE CASE 2.1 MEMO 1303.0 COORDINATE $\sim \theta_2$

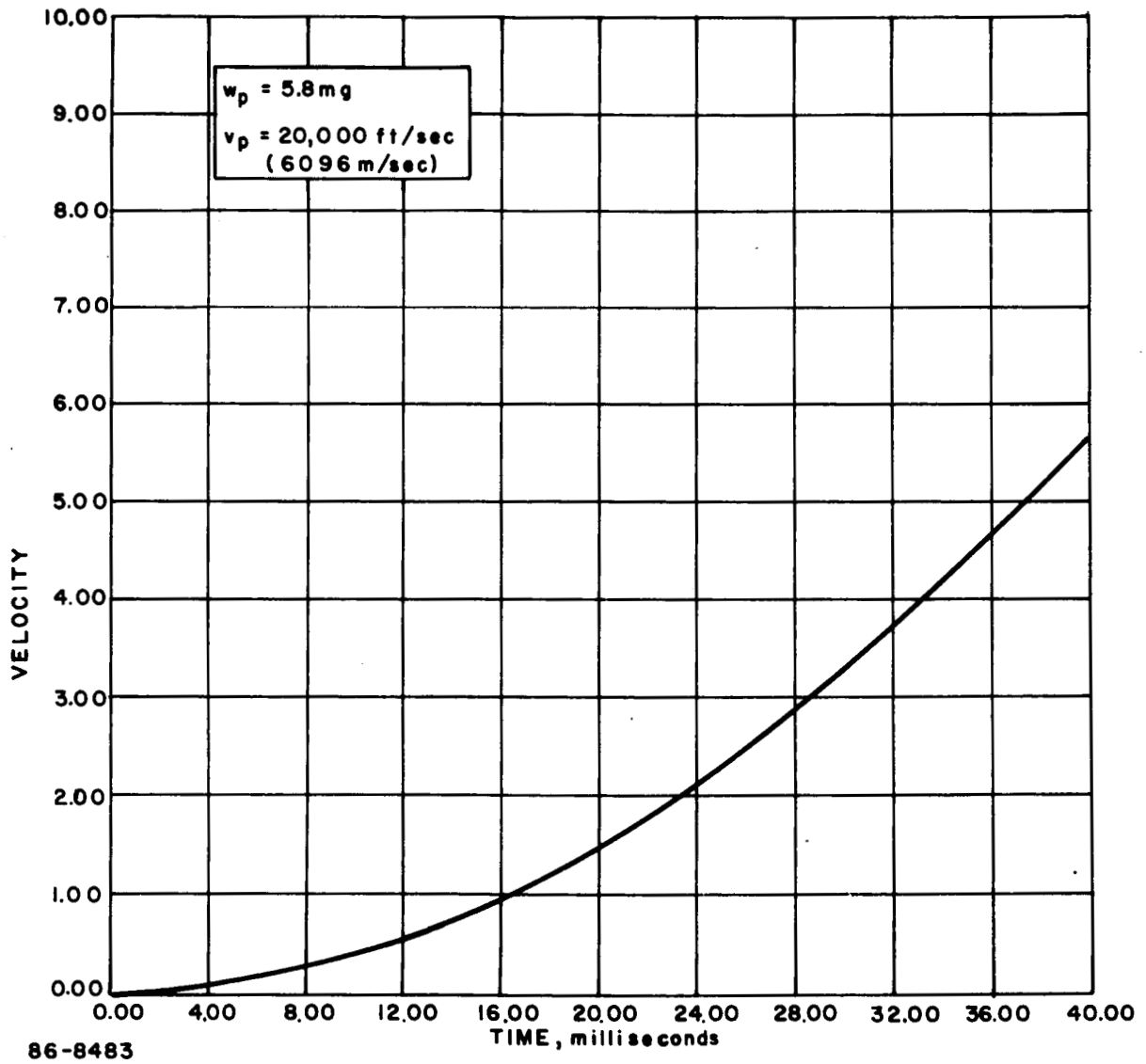


Figure A14 TRANSIENT RESPONSE CASE 2.1 MEMO 1303.0 COORDINATE $\sim \dot{\theta}_2$

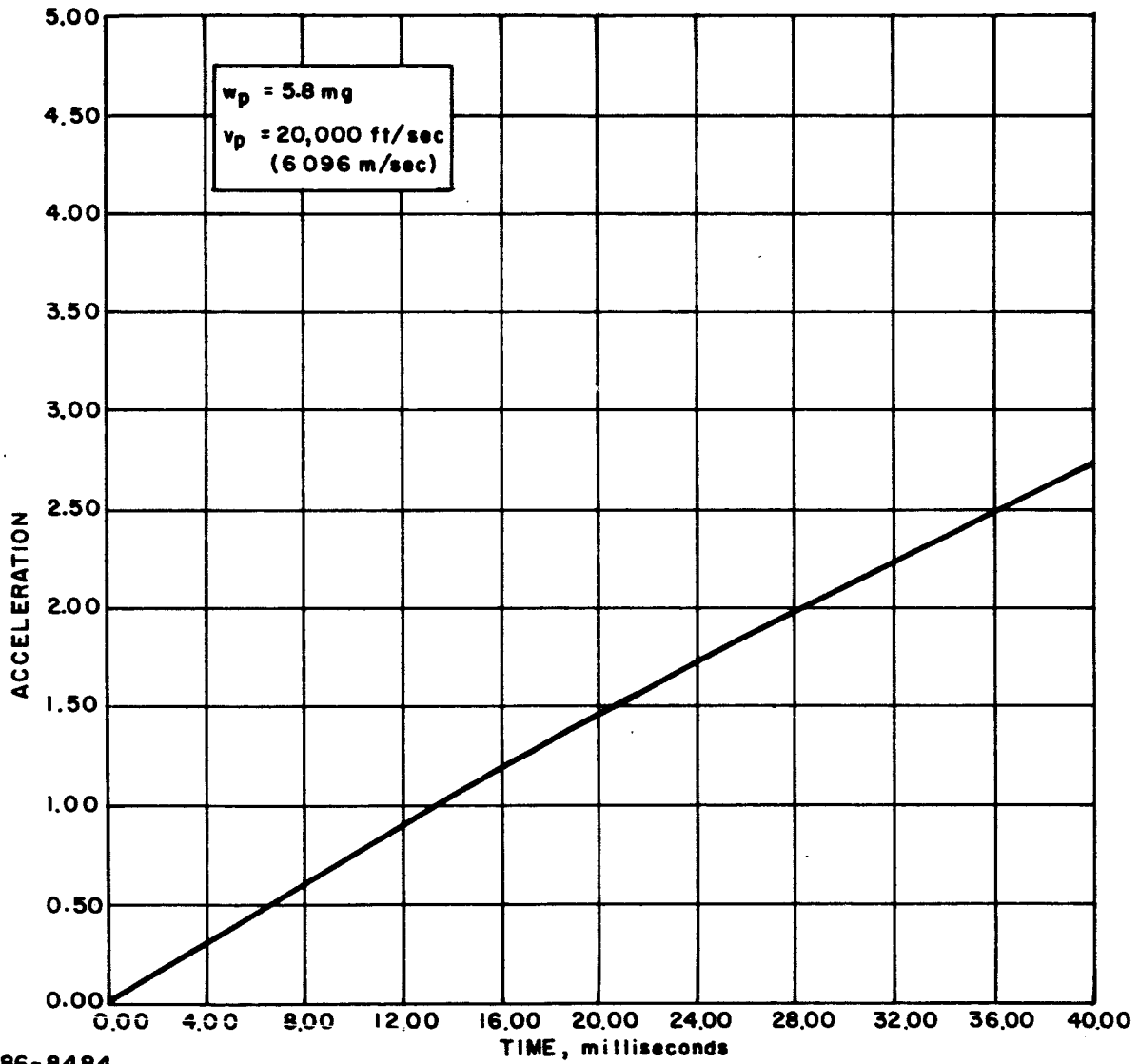


Figure A15 TRANSIENT RESPONSE CASE 2.1 MEMO 1303.0 COORDINATE $\sim \ddot{\theta}_2$

DISTRIBUTION

<u>Addressee</u>	<u>No. of Copies</u>
NASA Langley Research Center Langley Station Hampton, Virginia 23365 Attn: Contracting Officer	1
Edwin T. Kruszewski	15
Library, Mail Stop 185	1
R. L. Zavasky, Mail Stop 107	1
NASA Ames Research Center Moffett Field, California 94035 Attn: Library	1
NASA Flight Research Center P. O. Box 273 Edwards, California 93523 Attn: Library	1
NASA Goddard Space Flight Center Greenbelt, Maryland 20771 Attn: Library	1
Jet Propulsion Laboratory 4800 Oak Grove Drive Pasadena, California 91103 Attn: Library	1
NASA Manned Spacecraft Center Houston, Texas 77001 Attn: Library	1
NASA Marshall Space Flight Center Huntsville, Alabama 35812 Attn: Library	1
NASA Western Operations 150 Pico Boulevard Santa Monica, California 90406 Attn: Library	1
NASA Wallops Station Wallops Island, Virginia 23337 Attn: Library	1

DISTRIBUTION (Concl'd)

<u>Addressee</u>	<u>No. of Copies</u>
NASA Electronics Research Center 575 Technology Square Cambridge, Massachusetts 02139 Attn: Library	1
NASA Lewis Research Center Mail Stop 3-7 2100 Brookpark Road Cleveland, Ohio 44135	1
NASA John F. Kennedy Space Center Kennedy Space Center, Florida 32899 Attn: Code ATS-132	1
NASA Michoud Assembly Facility P. O. Box 26078 New Orleans, Louisiana 70126 Attn: Mr. Henry Quintin Code I-Mich-D	1
National Aeronautics and Space Administration Washington, D. C. 20546 Attn: Library, Code USS-10 Code RV Melvin G. Rosche, Code RV-2	1 1 1
NASA Scientific and Technical Information Facility P. O. Box 33 College Park, Maryland 20740 (+1 reproducible)	67
Research Library - Wilmington (+1 reproducible)	3
Research Library - Lowell (+1 reproducible)	1
Reports Distribution Center	50